The 16th National Day on Biomedical Engineering

Theme: ***Man and Machine***

FRIDAY, December 1st 2017
Royal Academy Palace, Hertogsstraat 1, 1000 Brussels

08h30 Registration and poster setup + coffee
09h00 Welcome by Sabine Van Huffel
09h15 Keynote lecture 1 by by **Heike Vallery**
Compliant Robotics for Human Augmentation: Towards Bio-Surpassing Functionality
09h45 Single slide poster presentations Part I hosted by Prof. Stefaan Vandenberghe
10h10 Keynote lecture 2 **Bram Vanderborgt**
Actuate2Assist
10h40 Coffee break + poster session
11h10 Keynote lecture 3 by **Pascal Doquet**
Neurostimulation: breakthrough technologies to address the patient needs
11h40 Single slide poster presentations Part II hosted by Prof. Stefaan Vandenberghe
12h05 Keynote lecture 4 by **Hendrik Lambert**
Spinal Cord stimulation to let paralyzed people walk again: is a dream turning in reality?
12h35 Lunch + poster session + industry stands at poster booth
13h45 Parallel sessions
16u00 Poster awards and drinks
16u30 End

Program parallel sessions

13h45	**General Introductory session (Auditorium Albert II)**	
	Rubens Room (sli.do #8064)	**Auditorium Albert II (sli.do #3871)**
14h00	"To PhD or not to PhD?", Stefaan Vanden Berghe & Philippe Lefèvre	"International Biomedical career", Hendrik Lambert
14h30	Successful start-ups/spin-offs in the field of Biomedical Engineering: Molecubes	"To see is to innovate, to innovate is to see", Jelle De Smet
15h00	Demos: Cochlear	Successful start-ups/spin-offs in the field of Biomedical Engineering: Byteflies
15h30	Demos: Siemens	"Biomedical engineer careers @government &healthcare"

Questions or remarks: info@ncbme.be
Website: www.ncbme.be
Facebook page: ncbmebelgium

Organized by the youngster committee: Florian Salmen, Simon Van Eyndhoven, Dario Farotto, Gerlinde Logghe, Vincent Van Eeghem, Ghazal Adeli Koudehi, Vicente Acuna, Benyameen Keelson

Sponsors of the poster awards

Keynote Speakers

Prof. dr. ir. Heike Vallery
TU Delft

Prof. dr. ir. Bram Vanderborght
VUB

Dr. ir. Pascal Doguet
Synergia Medical

Prof. dr. ir. Hendrik Lambert
G-Therapeutics

Keynote lecture 1 by Prof. dr. ir. Heike Vallery

Heike Vallery received her Dipl.-Ing. degree in Mechanical Engineering (with honors) from RWTH Aachen University in 2004 and her Dr.-Ing. in robotics from the Technische Universität München in 2009, where she had worked on compliant actuation and cooperative control principles for gait rehabilitation robots. As a postdoctoral fellow at ETH Zürich, she continued this research and developed mechatronic principles for cooperative human-robot interaction. From 2011 to 2012, she worked at Khalifa University Abu Dhabi as an assistant professor. Today, she holds an associate professorship at TU Delft. H. Vallery has published more than 60 peer- reviewed publications, filed 7 patent applications, and received diverse fellowships and awards, like the 1st prize of the euRobotics Technology Transfer Award 2014, a Vidi fellowship in 2016 from NWO, and the Henk-Stassen Award for Best Young Researcher BME 2017.

Keynote lecture 2 by Prof. dr. ir. Bram Vanderborght

Professor in Robotics at the Vrije Universiteit Brussel and member of the Brussels Human Robotic research center (www.brubotics.eu). He performed research stays in AIST, Tsukuba, Japan and IIT, Italy. He investigates soft and variable impedance actuators for applications in human-robot interaction like prostheses, exoskeletons, coworkers, legged robots and social robots. He received an ERC Starting Grant on Series-Parallel Elastic Actuation for Robotics (SPEAR). He is EiC of Robotics & Automation Magazine and member of the Flemish Young Academy.

Keynote lecture 3 by Dr. ir. Pascal Doguet

Pascal Doguet holds a PhD in electronics from the UCLouvain, Belgium. During his thesis, he was involved in the development of a visual prosthesis, designing the prosthesis electronics and application specific integrated circuits. He has expertise in electronics, custom integrated circuit design, software and firmware development, materials for implants and knowledge of quality control and regulatory affairs. He previously worked at Neurotech SA and was in charge of the R&D department and responsible for the development of their range of neurostimulators for epilepsy, sleep apnea and deep brain stimulation that he entirely designed. Driven by challenges, he is now the co-founder of the company Synergia Medical where he goes on developing state of art medical devices including implantable neurostimulators. He also has extensive experience in coordinating research projects at national and international levels.

Keynote lecture 4 by Prof. dr. ir. Hendrik Lambert

Hendrik Lambert holds a Master in Electronic Engineering and a Master in Biomedical Engineering from the University of Ghent, and obtained a PhD in Biomedical Engineering (Cum Lauda) from the same university. Meantime he has 20 years of international experience in the development of Medical Device technologies in small and large industries. All technologies were early stage, innovative and high risk technologies for treatment of cardiac, vascular and neurological diseases. Several of those technologies evolved into mature therapies that are used today worldwide as a standard of care. Clinical research associated with these developments led to several milestone publications on which he co-authors. In his function as Regulatory Affairs Manager, he was leading interactions with regulatory agencies worldwide, including FDA.

Currently he is Vice President of Clinical and Regulatory Affairs at G-Therapeutics, a startup company specialized in the development of neuromodulation devices of which he is a co-founder. The company is based in Eindhoven (NL) and in Lausanne (CH).

He is part-time Teaching Professor at the University of Ghent related to Safety and Regulations.

Abstracts Participants

Part I

Artificial Organs and Implants

ArtOrg1	Acuña	Vicente	Design methodology of inductive power transfer in implants
ArtOrg2	Rummens	Tim	Postoperative monitoring of tibial implant stability: soft tissue characterization

Bionics and Assistive Devices

AssisDev1	Dieudonné	Benjamin	Sound processing for listeners with a cochlear implant in one ear and a hearing aid in the other: making them able to localize sounds
AssisDev2	Fricke	Simone	Performance-based adaptive assistance for different subtasks of walking in LOPES II
AssisDev3	Somers	Ben	Neural entrainment to the speech envelope with a cochlear implant
AssisDev4	Vasiliauskaite	Egle	Selective laser sintered ankle foot orthosis can support drop foot gait

Medical/clinical engineering

MedEng1	Blanc	Loïc	Low melting point materials as controllable stiffness mechanism for endoscopic and catheter application
MedEng2	Canè	Federico	From 4D medical images (CT, MRI, Ultrasound) to 4D structured mesh models for patient-specific flow simulations in the human heart
MedEng3	Filtjens	Benjamin	Assessment of a mobile platform for monitoring gait
MedEng4	Goossens	Quentin	The use of a pneumatic broach to follow up implant insertion in cementless THA – an in vitro study
MedEng5	Hamelmann	Paul	Fetal heart rate measurements using a flexible ultrasound Sensor matrix
MedEng6	Huberland	François	Endomagnet: magnetic compression anastomosis by therapeutic endoscopy

Medical imaging

MedIma1	Christiaen	Emma	Functional connectivity changes during epileptogenesis: a longitudinal rs-fMRI study
MedIma2	Decuyper	Milan	Brain tumour classification using deep features from structural MRI
MedIma3	Huang	Yizhou	Ultrasound-based strain mapping for quantitative characterization of uterine activity outside pregnancy
MedIma4	Keelson	Benyameen	4D-CT for musculoskeletal applications: impact of scan protocol on image registration, motion estimation and radiation dose
MedIma5	Pétré	Maxime	Endoruler: a real-time measurement system in endoscopy
MedIma6	Turco	Simona	Pharmacokinetic modeling of targeted microbubbles: applications in angiogenesis imaging and therapy monitoring
MedIma7	Van Sloun	Ruud	Sparsity-driven super-resolution in clinical contrast-enhanced ultrasound
MedIma8	Wildeboer	Rogier	Estimation of dispersion and convection in three-dimensional contrast ultrasound imaging for prostate cancer localization

Part II

Biomechanics

Bmech1	Adeli Koudehi	Ghazal	Computational modeling of the lymphatic uptake
Bmech2	Chen	Shengda	Characterization of biomechanical properties of porcine mitral valve chordae tendineae
Bmech3	De Raeve	Eveline	Robotic motion simulator for testing orthopedic and prosthetic devices
Bmech4	Logghe	Gerlinde	Propagation-based phase-contrast synchrotron imaging of aortic dissection in mice: from individual elastic lamella to 3D analysis
Bmech5	Mancini	Viviana	Prediction of post stenotic flow instabilities in a patient-specific common carotid artery model
Bmech6	Rocatello	Giorgia	Low implantation depth during TAVR increases the pressure exerted on the atrioventricular conduction system: a biomechanical analysis
Bmech7	Tommasin	Daniela	Biomechanics of wave propagation through hydrogels mimicking soft biological tissues
Bmech8	Van Hulle	Romain	Estimation of ground reaction forces based on kinematic data

Biosignals

Bsign1	Boutaayamou	Mohamed	A gait cycle partitioning method using a foot-worn accelerometer system
Bsign2	Deviaene	Margot	Detecting cardiovascular comorbidities in sleep Apnea patients using SpO2
Bsign3	De Wel	Ofelie	The evolution of EEG complexity during brain maturation in preterm infants using multiscale entropy
Bsign4	Ebrahimbabaie	Pouyan	Geometric Brownian Motion (GBM) as a promising random process model of the time evolution of the level of drowsiness
Bsign5	Ebrahimbabaie	Pouyan	Effectiveness of Geometric Brownian Motion (GBM) random process model for modelling the PRECLOS signals of narcoleptic subjects
Bsign6	Fredy Morales	Johan	A method for sleep Apnea Hypopnea syndrome classification in SpO2 signals
Bsign7	Hendrikx	Dries	Assessment of the effects of propofol on the cerebral hemodynamic regulation mechanisms of the premature neonates using graphs
Bsign8	Huysmans	Dorien	Unsupervised learning for mental stress detection - exploration of self-organizing maps
Bsign9	Lavanga	Mario	An EEG maturation study based on multifractality in preterm neonates
Bsign10	Padhy	Sibasankar	Irregular heartbeat classification using multiscale tensor analysis
Bsign11	Vandecasteele	Kaat	Epileptic seizure detection based on wrist Photoplethymography (PPG): detection of noise segments
Bsign12	Van Eyndhoven	Simon	Identifying neurovascular coupling in brain networks through structured matrix-tensor factorization of EEG-fMRI data
Bsign13	Villa Gómez	Amalia	A tool for automatic heartbeat classification in ambulatory ECG

Bsign14	Zhang	Yiyuan	A Review on wearable sensors for age-related frailty

Artificial organs and implants

DESIGN METHODOLOGY OF INDUCTIVE POWER TRANSFER IN IMPLANTS

Vicente Acuña[1*], Adrien Debelle[1], Laurent Lonys[1], Antoine Nonclercq[1]

[1]Université libre de Bruxelles, BEAMS Department, Belgium

Keyword(s): bioelectronics and photonics, artificial organs and implants

1. INTRODUCTION

Battery life in implanted stimulators is a common limiting factor. Indeed, stimulators deliver a large amount of power with a restricted power source. It is therefore necessary to pay attention to power efficiency. Inductive power transfer (IPT) is a widespread solution to power, recharge or communicate with an implanted medical device without percutaneous driveline that can produce infections.

The main challenge in the design of IPT systems results from the low magnetic coupling between both coils. The efficiency is related to the coupling coefficient *k*, which is in turn related to the position of the coils (affects the mutual inductance) and the Quality factor of each coil. A higher quality factor means lower energy losses in comparison to the stored energy. To increase the efficiency, the coils used in the wireless system are operating in a resonant converter topology.

This paper presents a tool to design an IPT system for implants. It will be first illustrated in the case of a subcutaneous implantable gastrostimulators, helping obese patients to lose weight, proposed by our group [1], but also for deeply implanted devices, to compare the methodology for different applications.

2. MATERIALS AND METHODS

To design an IPT system, various design considerations need to be taken into account, namely the size of the implant (restricting the size of the coil), the implant location, and the power consumption. Based on these, our tool aims to give the best design in terms of efficiency, power transfer, or gain.

One of the major challenges consists in defanging the best dimensions and configuration of external and implanted coils. Our tool includes a 2D or 3D finite element model that maximises the coupling, based on design considerations,

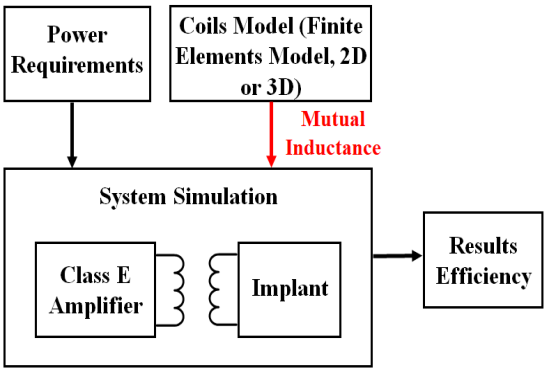

Figure 1. Block diagram of the wireless transfer system.

informing this way of the resulting geometry of these and the spacing in the windings.

3. RESULTS AND DISCUSSION

The tool is able to optimise, for a given implant, the IPT of the global system, or to focus on a given part of it, such as the dimensions and configuration of external and implanted coils.

For instance, with the finite elements model, it is possible to know the differences in the mutual inductance and current induced in the secondary coil, when modifying the geometry of the primary coil. For example, two coils that show L1= 319 uH and L2= 9.11 uH, for a given “standard” winding at the primary coil, present a mutual inductance of 11.4 uH. Increasing slightly spacing between the windings of the primary coil also increases the mutual inductance to 11.6 uH, which affects in turn the coupling coefficient and the efficiency of the global system. Different configurations can therefore be compared to choose the best design.

References

[1] Lonys L. et al. Design and Implementation of a Less Invasive Gastrostimulator. *European journal of translational myology*, 26(2), 6019, 2016.

POSTOPERATIVE MONITORING OF TIBIAL IMPLANT STABILITY: SOFT TISSUE CHARACTERIZATION

Rummens T[1*], Goossens Q[1], Pastrav L[1], Vandenneucker H[2], Desmet W[3], Vander Sloten J[4], Denis K[1], Labey L[4]

[1]KU Leuven, Department of Mechanical Engineering, Smart Instrumentation, Belgium
[2]KU Leuven, Department of Development and Regeneration – Orthopaedic Surgery UZ Leuven, Belgium
[3]KU Leuven, Department of Mechanical Engineering, PMA Section, Belgium
[4]KU Leuven, Department of Mechanical Engineering, Biomechanics Section, Belgium
[5]KU Leuven, Mechanical Engineering Technology TC, Geel, Belgium

Keyword(s): medical/clinical engineering – artificial organs and implants

1. INTRODUCTION

The aim of this project is to develop a non-destructive vibration-based technique to aid the postoperative assessment of loosening of the tibial component of a total knee arthroplasty.

Preliminary tests on artificial bones indicated that loosening of the tibial component can be detected by extraction of several vibrational features [1]. However, to bring this technique into clinical practice, it is necessary to cope with soft tissue (e.g. skin, adipose tissue and ligament).

Soft tissue, being a viscoelastic material, will dampen the vibration signal. The amount of energy loss depends on the frequency of the signal. To find a frequency range usable for loosening feature extraction, a test setup is built and high frequency characterization of TKR relevant tissue is attempted.

2. MATERIALS AND METHODS

Two methods are used for obtaining the complex modulus and loss factor of porcine skin over a wide frequency range. The first method obtains these parameters from the resonance frequency of the system. By shifting this frequency via changing the mass of the (one degree-of-freedom) system, a number of frequencies can be characterized. The second method obtains these parameters from the transmissibility and phase between two accelerometers. Both methods use the same setup. The setup contains an electrodynamic shaker (A), impedance head (B), bottom plate (C), soft tissue sample (D), top mass (E) and an accelerometer (F) on top. To keep the soft tissue from dehydrating, a saline is used around the edge of the sample.

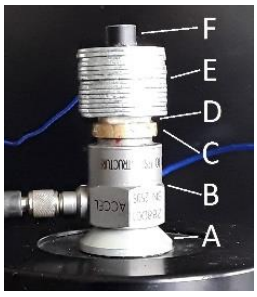

Figure 1: The test setup

3. RESULTS AND DISCUSSION

Results of both methods show that porcine skin, when analyzed over a frequency range from 100 to 1000Hz, has a rising loss factor with a maximum increase at 700Hz. Thus the loss modulus (i.e. the materials ability of dissipating energy) becomes more important at frequencies above 700Hz. Additionally, keeping the sample hydrated has an important effect on the reproducibility of the test.

However, because of the moisture of soft tissue, it is difficult to attach the sensor equipment, while keeping the sample hydrated. Preparing the samples with a uniform thickness and dissecting it from the underlying tissue layers is also a complicated operation.

More effort is needed into optimizing the sample preparation. Additionally, future work will focus on improving the test setup for working with biological samples.

References

[1] Leuridan S. et al. Vibration-based fixation assessment of tibial knee implants: A combined in vitro and in silico feasibility study. *Med Eng Phys,* 49, 109-120, 2017.

Bionics and assistive devices

SOUND PROCESSING FOR LISTENERS WITH A COCHLEAR IMPLANT IN ONE EAR AND A HEARING AID IN THE OTHER: MAKING THEM ABLE TO LOCALIZE SOUNDS

Benjamin Dieudonné[1]*, Tom Francart[1]

[1]KU Leuven, Department of Neurosciences, ExpORL, B-3000 Leuven, Belgium.

Keyword(s): bionics and assistive devices

1. INTRODUCTION

An increasingly common solution to severe hearing loss is bimodal stimulation: a cochlear implant in one ear and a hearing aid in the other [2,3]. A hearing aid restores hearing by sound amplification; a cochlear implant is surgically implanted and restores hearing by electrical stimulation of the auditory nerve.

Bimodal listeners struggle with localizing sounds, an important skill to be able to participate in conversations in social environments such as a party or a restaurant. For example, to be able to localize a sound coming from the left, it should be perceived louder and/or earlier at the left ear than at the right. However, with the current sound processing of the devices, bimodal listeners barely perceive these so-called interaural level and time differences.

Many researchers have already developed sound processing strategies to enhance the transmission of interaural level and time differences for hearing impaired listeners [1,2,3,4]. Unfortunately, these strategies are computationally cumbersome and therefore not suitable for application in current clinical devices.

We present a new method that does not require complex processing, to exaggerate interaural level differences for bimodal listeners.

2. MATERIALS AND METHODS

We supply both devices with a fixed acoustic beamformer, such that they amplify sounds coming from their own side, and attenuate sounds coming from the other side. For example, a sound coming from the cochlear implant side is amplified in the cochlear implant and attenuated in the hearing aid, resulting in an interaural level difference.

Each acoustic beamformer is achieved with a microphone array consisting of one microphone per device and a link between the devices.

3. RESULTS AND DISCUSSION

Our method significantly improved sound localization performance in acoustic simulations of bimodal listening. The method is also promising to improve speech understanding in noisy environments. Due to its low computational complexity, the method is suitable for application in current clinical devices.

4. REFERENCES

[1] Brown, C.A. Binaural enhancement for bilateral cochlear implant users. *Ear and hearing*, 35(5), 580, 2014.

[2] Francart, T., Lenssen, A., and Wouters, J. Enhancement of interaural level differences improves sound localization in bimodal hearing. *The Journal of the Acoustical Society of America*, 130(5), 2817-2826, 2011.

[3] Francart, T., Lenssen, A., and Wouters, J. Modulation enhancement in the electrical signal improves perception of interaural time differences with bimodal stimulation. *Journal of the Association for Research in Otolaryngology*, 15(4), 633-647, 2014.

[4] Moore, B. C., Kolarik, A., Stone, M. A., and Lee, Y. W. Evaluation of a method for enhancing interaural level differences at low frequencies. *The Journal of the Acoustical Society of America*, 140(4), 2817-2828, 2016.

PERFORMANCE-BASED ADAPTIVE ASSISTANCE FOR DIFFERENT SUBTASKS OF WALKING IN LOPES II

Cristina Bayón[1], Simone Fricke[2*], Herman van der Kooij[2], Edwin van Asseldonk[2]
[1]Centro de Automática y Robótica, CAR-CSIC, Spain
[2]Department of Biomechanical Engineering, University of Twente, The Netherlands

Keyword(s): biomechanics – bionics and assistive devices

1. INTRODUCTION

Robotic gait training is a promising tool to improve walking ability after stroke, however, therapeutic effect might largely depend on the type of robotic gait trainer and control algorithm that is used [1]. Therapy should be task-specific and promote active participation as this is crucial for motor learning. Some algorithms have been proposed to encourage patients to actively participate [2], however, the amount of assistance for different subtasks of the gait cycle is chosen by the therapist, and therefore, therapy could be affected by subjective decisions.

This contribution presents a novel controller that is able to automatically adapt the assistance for specific subtasks of gait based on patients' performance. This approach is expected to improve robotic gait therapy.

2. MATERIALS AND METHODS

2.1 Robotic platform

LOPES II was used to develop and test the algorithm. LOPES II is a treadmill-based, admittance controlled robotic gait trainer that has eight actuated degrees of freedom to control the motion of the lower limbs and pelvis [2].

Currently, LOPES II is 'manually' controlled through a graphical user interface in which the operator can adjust the level of support for several gait subtasks (i.e. step length, step height, stance, prepositioning and weight shift).

2.2 Adaptive controller

A new adaptive controller that is able to automatically change the assistance provided to the patient has been developed. The controller evaluates patients' performance with respect to reference values in a defined number of preceding steps. This evaluation is done for each subtask of walking separately. Based on this, the assistance is automatically adjusted for each subtask of gait and might be affected in different ways: first, if performance is within a specific range around a previously selected threshold, amount of assistance in the particular subtask will remain constant; and second, assistance will be increased or decreased depending on whether the performance is below or above the specified range respectively.

3. RESULTS AND DISCUSSION

A preliminary evaluation of the algorithm in healthy users showed the potential of the controller to adjust the assistance for different subtasks of gait depending on the user's needs. (e.g. simulated stiff knee gait resulted in increased assistance in step height or knee flexion; meanwhile simulated crouch gait was corrected providing assistance in knee and hip extension).

In coming studies, authors plan to validate the algorithm in stroke survivors in two ways: First, to evaluate its benefits compared to the current 'manual' assistance where the operator selects the amount of support; and second, to study the effect of different amounts of body weight support and walking speed on the amount of assistance provided by the algorithm.

In the future, an optimized version of this algorithm might not only improve robotic gait training for stroke survivors, but could also be used for assessment of patients' abilities and to monitor progress during rehabilitation.

References

[1] Pennycott, A. et al. Towards more effective robotic gait training for stroke rehabilitation: a review. *Journal of neuroengineering and rehabilitation,* 9(1), 65, 2012.

[2] Meuleman, J. et al. LOPES II - Design and Evaluation of an Admittance Controlled Gait Training Robot with Shadow-Leg Approach. *IEEE transactions on neural systems and rehabilitation engineering,* 24(3), 352-363, 2016.

NEURAL ENTRAINMENT TO THE SPEECH ENVELOPE WITH A COCHLEAR IMPLANT

Ben Somers[1*], Eline Verschueren[1], Jan Wouters[1], Tom Francart[1]
[1]KU Leuven – University of Leuven, Department of Neurosciences, ExpORL, Belgium

Keyword(s): biosignals, bionics and assistive devices

1. INTRODUCTION

A cochlear implant (CI) is an auditory prosthesis that restores the hearing function in patients with severe hearing impairment of deafness through direct electrical stimulation of the auditory nerve. Studies with normal-hearing participants have shown that the temporal envelope of speech is encoded in oscillating patterns of the listener's brain [1,3]. This neural representation of the envelope can be decoded from neural recordings [2], and its strength is related to speech intelligibility [4]. It is hypothesized that this response is also present with electrical speech stimulation. However, this response is difficult to measure, because electrical stimulation artifacts hamper EEG recordings in CI users. In this study, neural entrainment to the speech envelope using EEG is demonstrated for the first time in CI users.

2. MATERIALS AND METHODS

EEG was measured from CI users while they listened to natural running speech. A novel technique to suppress the electrical stimulation artifacts is applied during preprocessing. Using a cross-validation approach, a part of the artifact-free EEG is used to train a linear decoder, which reconstructs the speech envelope from the EEG by optimally combining the time signals from multiple channels. The decoder is then applied to the remaining EEG to reconstruct the envelope. The strength of neural entrainment to the envelope is measured by correlating the reconstructed envelope with the real envelope. To validate that the EEG is free of components related to the electrical stimulation, the same decoder is applied to EEG measured while the subject is stimulated below threshold level. EEG obtained during sub-threshold stimulation still contains electrical artifacts, but is free of neural response to the stimulus.

3. RESULTS AND DISCUSSION

The correlation between reconstructed and real speech envelope was significant above chance level, indicating that there is neural entrainment to the speech envelope. The envelope reconstructed from sub-threshold stimulation did not correlate with the real envelope, indicating that the electrical artifacts, if at all, only have a minor contribution to the significant responses.

In conclusion, this study demonstrates that neural entrainment to the speech envelope can be measured as a response to electrical stimulation. Reliable EEG recordings for experimental purposes were obtained using a novel CI artifact suppression technique. It was verified that the responses to the speech envelope are of neural origin and that the electrical artifacts do not affect the envelope reconstruction. The demonstrated measure for the neural encoding of speech may support future automatic fitting methods and other objective measures of hearing with a CI.

References

[1] Aiken, S.J. and Picton, T.W. Human cortical responses to the speech envelope. *Ear and hearing*, 29(2), 139-157, 2008.

[2] Ding, N. and Simon, J.Z. Adaptive temporal encoding leads to a background-insensitive cortical representation of speech. *Journal of Neuroscience*, 33(13), 5728-5735, 2013

[3] Peelle, J. E. and Davis, M. H., Neural oscillations carry speech rhythm through to comprehension. *Frontiers in psychology*, 3, 320, 2012

[4] Vanthornhout, J. et al. Speech intelligibility predicted from neural entrainment of the speech envelope. *Manuscript in review*.

SELECTIVE LASER SINTERED ANKLE FOOT ORTHOSIS CAN SUPPORT DROP FOOT GAIT

Egle Vasiliauskaite[1,2*], Alessio Ielapi[2], Jan Deckers[3], Miguel Vermandel[3], Matthieu De Beule[2], Wim Van Paepegem[4], Malcolm Forward[1,2], Frank Plasschaert[1]

[1]Ghent University, Department of Physical Medicine and Orthopaedic Surgery
[2]Ghent University, Department of Electronics and Information Systems, IbiTech-bioMMeda
[3]V!go Group N.V., Belgium
[4]Ghent University, Department of Materials Science and Engineering

Keyword(s): medical/clinical engineering – assistive devices

1. INTRODUCTION

Drop foot gait – is a walking pattern that is initiated with the forefoot or toes, rather than the heel. It can be a consequence of a medical condition or trauma. Problems associated with the drop-foot gait are: increased risk of tripping; increased energy demands.

An ankle-foot-orthosis (AFO) is an assistive device that has potential to prevent drop foot gait, make walking more energy efficient and safer. To achieve these goals AFO mechanical characteristics, e.g. ankle stiffness, should be tuned to individual patient needs. However, to date there are no quantitative guidelines for AFO stiffness prescription and there are no quantitative methods to control AFO mechanical characteristics. Advances in additive manufacturing and motion tracking technology together create the potential to change this situation.

The aim of this study was to compare the influence of the thermoformed and additively manufactured AFO on the drop-foot gait.

2. MATERIALS AND METHODS

A patient with drop-foot gait pattern was considered in this case study. Two types of custom orthoses were produced: thermoformed polypropylene orthosis (AFO-PP) and selective laser sintered polyamide orthosis (AFO-PA). Ankle stiffness of both orthoses was measured in a dedicated AFO testing rig. The impact of the AFO on the patients' gait was assessed in the gait laboratory.

3. RESULTS AND DISCUSSION

AFO-PA was found to be stiffer than AFO-PP. Both AFO types had positive and similar impacts on patients' gait: (1) both restored heel strike foot pattern and ensured clearance in the swing phase (2) both increased walking speed compared to barefoot or shoes only walking. The results suggest that patient was able to adapt to different AFO characteristics. The ability to adapt to different orthotic stiffness has been reported in the literature [1]. However, as in the present study, orthotic users expressed subjective preference for certain AFO stiffness.

Further investigations, e.g. musculoskeletal modeling, might reveal adaptation mechanisms and energetic costs involved in walking with different stiffness orthoses. This information is vital to aid patient specific prescription of AFO.

ACKNOWLEDGEMENTS

This research was funded by VLAIO, project numbers 140164 & 140165.

References

[1] Esposito, E.R., Choi, H.S., Owens, J.G., Blanck, R.V. and Wilken, J.M. Biomechanical response to ankle-foot orthosis stiffness during running. *Clin. Biomech.*, 3(10), 1125-1132, 2015.

Medical/Clinical engineering

LOW MELTING POINT MATERIALS AS CONTROLLABLE STIFFNESS MECHANISM FOR ENDOSCOPIC AND CATHETER APPLICATIONS

Loïc Blanc[1*], Alain Delchambre[2], Pierre Lambert[1]

[1]Université Libre de Bruxelles, Transferts, Interfaces et Procédés Departement, Belgium

[2]Université Libre de Bruxelles, BEAMS - Micro and Biomechanical Engineering, Belgium

Keyword(s): medical/clinical engineering

1. INTRODUCTION

During Minimally Invasive Surgery, the endoscopic devices need to be sufficiently flexible to avoid damaging patient tissues or causing pain, but they also have to be stiff enough to transmit force during punctures and grasping tasks or for supporting other tools. Several controllable stiffness solutions have been highlighted in the literature [1]. This work focuses on Low Melting Point Materials that show an important change in mechanical properties when they are heated around their transition temperature. This study is focused on the scaling laws of such solutions for catheter applications (with diameters below 3mm), on the mechanical rules of design and on the stiffness performances.

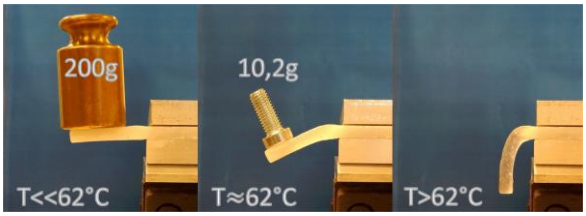

Figure 1: Stiffness transition between rigid (left) and flexible (right) states for a polycaprolactone sample.

2. MATERIALS AND METHODS

Several materials with a low melting point are compared in this study (Low Melting Point Metal such as gallium and Low Melting Point Polymer such as polycaprolactone). The stiffness gain between the rigid and the flexible states ranges from two to four orders of magnitude. First, the mechanical characterization of these materials is performed on simplified shapes to observe the influence of the manufacturing process, the dimensions and the working conditions. The tests are performed at room temperature (rigid state) and at higher temperature (flexible state) in order to characterize the samples thermo-mechanically. For the flexible-state tests, hot air is blown on the samples to change their mechanical properties due to a change of temperature. Other heat transmission solutions are studied to find the most suitable and efficient method for medical devices applications.

3. RESULTS AND DISCUSSION

The first proof of concept based on these materials shows encouraging performances. The strong change in stiffness of polycaprolactone samples around the melting temperature (62°C) is illustrated in Figure 1. The gallium-based solution presents a very large change in stiffness around a lower melting temperature (~ 30°C).

The fabrication of devices corresponding to the targeted applications is still under study. The manufacturing of small structures (diameters <3mm) is challenging. First, a large scale design is implemented as proof of concept and its thermo-mechanical response is studied. The ease of manufacturing, the production reproducibility, the thermal efficiency, the safety aspects and the stiffness performances have to be taken into account for the validation step. The current tests have showed promising results. Further characterization and study of the design have to be performed to reach the goals targeted by the application. Several other materials with different mechanical properties may be used in a similar approach. A simplified thermo-mechanical model is under construction to simplify the design. This work was supported by the F.N.R.S. through an F.R.I.A. grant.

References

[1] Blanc, L., Delchambre, A. and Lambert, P. Flexible Medical Devices: Review of Controllable Stiffness Solutions," *Actuators*, vol. 6, no. 23, 2017. Multidisciplinary Digital Publishing Institute.

FROM 4D MEDICAL IMAGES (CT, MRI, ULTRASOUND) TO 4D STRUCTURED MESH MODELS FOR PATIENT-SPECIFIC FLOW SIMULATIONS IN THE HUMAN HEART

Federico Canè[1*], Benedict Verhegghe[1,2], Matthieu De Beule[1,2], Philippe B. Bertrand[3], Rob J. van der Geest[4], Patrick Segers[1], Gianluca De Santis[2]

[1]IBiTech – bioMMeda, Department of Electronics and Information Systems, Ghent University, Ghent, Belgium; [2]FEops NV, Ghent, Belgium; [3]Department of Cardiology, Ziekenhuis Oost-Limburg, Schiepse Bos 6, 3600, Genk, Belgium; [4]Division of Image Processing, Department of Radiology, Leiden University Medical Center, Leiden, The Netherlands

Keyword(s): medical imaging – medical/clinical engineering

1. INTRODUCTION

Cardiovascular disease (CVD) remains the most important cause of death worldwide [1]. Risk stratification and early detection of abnormalities is essential, which implies a profound insight in and knowledge of the (patho)physiology of cardiovascular function. Intra-cardiac flow is an important component of ventricular function, where vortex formation has been shown to interplay with the function of valves, motion kinetics, wash-out of ventricular chambers and ventricular energetics [2]. Coupling between Computational Fluid Dynamics (CFD) simulations and medical images is still required to study intra-cardiac flow in sufficient temporal and spatial detail, and can play a fundamental role in terms of patient-specific diagnostic tools. From a technical perspective, CFD simulations with moving boundaries could easily lead to negative volumes errors and the sudden failure of the simulation. The generation of high-quality 4D meshes (3D in space + time) with 1-to-1 vertex becomes essential to perform a successive CFD simulation with moving boundaries. In this context, we developed a semi-automatic morphing tool able to create 4D high-quality structured meshes starting from a segmented 4D dataset.

2. MATERIALS AND METHODS

Our morphing tool was developed in PyFormex, a python-based open-source software environment. The general strategy behind the morphing tool is to cover the segmented surfaces of the 4D dataset [Figure 1.c] , which typically have a non-adequate quality of the surface mesh, with a patch [Figure 1.a] that has the desired mesh topology by means of isoparametric transformations. Therefore, by applying sequentially the isoparametric transformation [Figure 1.d], the patch containing the desired mesh topology is repetitively attached to the parts which compose the entire LV endocardial wall. Since it is impossible to mesh the LV as a whole, the semi-automatization process of the algorithm was performed by subdividing the LV in three different subdomains: the ventricular sac, the atrium and aorta, and the zone connecting both.

3. RESULTS AND DISCUSSION

The method was tested on three different 4D datasets (Ultrasound, MRI, CT) to prove its versatility. Both the quality and accuracy of the resulting 4D meshes were evaluated to assess the performance of the tool. Furthermore, an estimation of some physiological quantities was accomplished for the 4D CT reconstruction. Future research will aim at extending the region of interest by taking advantage of image fusion, further automation of the meshing algorithm and at generating structured hexahedral mesh models both for the blood and myocardial volume.

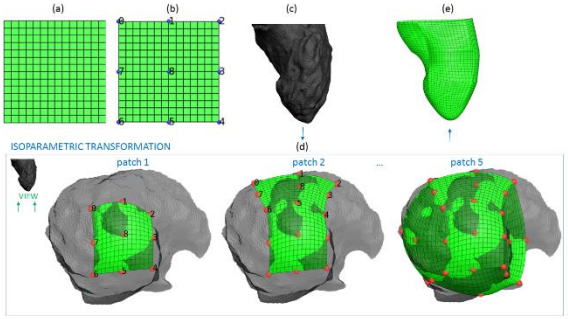

Figure 1

References

[1] WHO, Media Centre: Cardiovascular disease. WHO, vol.1, 1-6, 2015.

[2] Bavo, A.M. et al. Patient specific CFD simulation of intraventricular haemodynamics based on 3D ultrasound imaging. *Biomedical engineering online,* 15(1), 107, 2016.

ASSESSMENT OF A MOBILE PLATFORM FOR MONITORING GAIT

Benjamin Filtjens[1,2,3,4*], Robin Amsters[1,4], Ali Bin Junaid[1,4], Nick Damen[1], Jeroen Van De Laer[1], Bart Vanrumste[2,3], Peter Slaets[1,4]

[1]KU Leuven, Department of Mechanical Engineering, Belgium

[2]KU Leuven, Department of Electrical Engineering (ESAT), STADIUS – IMEC, Belgium

[3]KU Leuven, eMedia Research Lab, Belgium

[4]KU Leuven, Intelligent Mobile Platform Research Group, Belgium

Keyword(s): medical/clinical engineering

1. INTRODUCTION

Human gait analysis, defined as the study of human movement, is an important indicator of the physical and mental well-being of a person [1,2]. Gait data is therefore often used in diagnostics, general health monitoring, or for assessing a person's rehabilitation process. Existing gait analysis systems are either expensive, intrusive, or require structured environments such as a laboratory. In this research, a mobile platform is presented as a low-cost, unobtrusive method to continuously monitor gait in a person's natural environment.

2. MATERIALS AND METHODS

The data was gathered by tracking the joint movements, with a Microsoft Kinect, while following a person from a fixed distance. A total of 9 experiments were conducted in a controlled environment, 4 with a camera angle of 25° and 5 with a camera angle of 30°. To improve detection, the data was filtered with a Kalman filter for parameter estimation in real-time and a Rauch-Tung-Striebel (RTS) smoother in post processing. The gait parameters that were extracted by processing the filtered data are the step length, cycle time, and cadence (step cycles/min). The proposed approach was validated by using a VICON motion capture system.

3. RESULTS AND DISCUSSION

The results concluded a large offset in step length, while the step times could be detected with an average accuracy of around 10 milliseconds. By using a RTS smoother the offset in step length was reduced to 9%, as can be seen in figure 1, an average accuracy of a few centimeters. These results are comparable to existing works, despite the camera moving while tracking.

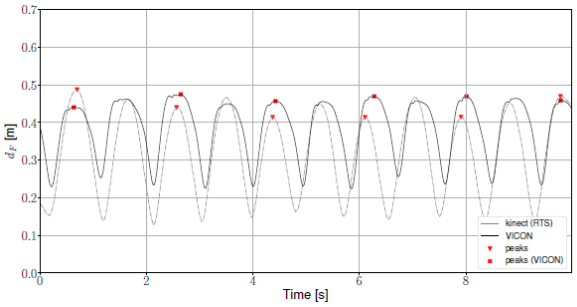

Figure 1: Feet distance based on Kinect measurements after RTS smoother (camera angle = 25°).

References

[1] Hausdorff, J., Rios, D. and Edelberg, H. Gait variability and fall risk in community-living older adults: A 1-year prospective study. *Archives of Physical Medicine and Rehabilitation,* 82(8), 1050-1056, 2001.

[2] Hodgins, D. The importance of measuring human gait. *Medical Device Technology,* 19(5), 42-44, 2008.

THE USE OF A PNEUMATIC BROACH TO FOLLOW UP IMPLANT INSERTION IN CEMENTLESS THA - AN IN VITRO STUDY

Quentin Goossens[1*], Matthias Rogiers[1], Matthias Vanbrabant[1], Leonard Pastrav[1], Steven Leuridan[2], Michiel Mulier[3], Wim Desmet[4], Kathleen Denis[1], Jos Vander Sloten[2]

[1]KU Leuven Campus Groep T, Smart Instrumentation, Belgium
[2]KU Leuven, Biomechanics Section, Belgium
[3]UZ Pellenberg, Department of Orthopedics, Belgium
[4]KU Leuven, PMA Section, Belgium

Keyword(s): biomechanics – medical/clinical engineering

1. INTRODUCTION

A large number of total hip arthroplasties (THA) are performed each year, of which 60 % use cementless femoral fixation. This means that the implant is press-fitted in the bone by hammer blows. The initial fixation is one of the most important factors for a long lasting fixation [1]. It is not easy to obtain the point of optimal initial fixation, because excessively press-fitting the implant by the hammer blows can cause peak stresses resulting in femoral fracture. In order to reduce these peak stresses during reaming, IMT Integral Medizintechnik (Luzern, Switzerland) designed the Woodpecker, a pneumatic broaching device using a vibrating tool. This study explores the feasibility of using this pneumatic broach for implant insertion and detection of optimal fixation by analyzing the vibrational response of the implant and the pneumatic broach. The press-fit of the implant is quantified by measuring the strain in the cortical bone surrounding the implant. An in vitro study is presented.

2. MATERIALS AND METHODS

Two replica femur models (4th generation #3403, Sawbones Europe AB, Malmo Sweden) were used in this study. One of the femur models was instrumented with three rectangular strain gauge rosettes (Micro-Measurements, Raleigh, USA). The rosettes were placed medially, posteriorly and anteriorly on the proximal femur. Five paired implant insertions were performed on both bone models, alternating between standard hammer blow insertions and using the pneumatic broach. The vibrational response was measured during the insertion process, at the implant and broach side using two shock accelerometers (PCB Piezotronics). The endpoint of insertion was defined as the point when the static strain stopped increasing.

3. RESULTS AND DISCUSSION

Peak stress values calculated from the strain measurement during the insertion showed to be significantly ($p < 0.05$) lower at two locations using the pneumatic broach compared to the hammer blows at the same level of static strain. However, the final static strain at the endpoint of insertion was approximately a factor two lower using the pneumatic broach compared to the hammer.

Significant trends were observed in the bandpower feature that was calculated from the acceleration measurement at the implant side during the pneumatic broach insertion. The bandpower is defined as the percentage power of the spectrum in the band 0-1000 Hz. A decreasing trend was observed, followed by a stagnation. This point of stagnation was correlated with the stagnation of the periprosthetic stress in the bone measured by the strain gages. The behavior of this bandpower feature shows the possibility of using vibrational measurements during insertion to assess the endpoint of insertion, which is currently challenging to achieve. However it needs to be taken into account that it was not possible to reach the same level of static strain using the pneumatic broach as with the hammer insertion. This could mean that either extra hammer blows or a more powerful pneumatic device could be needed for proper implant insertion.

References

[1] Gheduzzi S., Miles A. A review of pre-clinical testing of femoral stem subsidence and comparison with clinical data. *Proceedings of the Institution of Mechanical Engineers, Part H*, 221(1), 39-46, 2007.

FETAL HEART RATE MEASUREMENTS USING A FLEXIBLE ULTRASOUND SENSOR MATRIX

Paul Hamelmann[1*], Massimo Mischi[1], Rik Vullings[1], Alexander F. Kolen[2], Shivani Joshi[3], Judith O.E.H. van Laar[4] and Jan W.M. Bergmans[1]

[1]Eindhoven University of Technology, Electrical Engineering, The Netherlands
[2]Philips Research Eindhoven, The Netherlands
[3]Delft University of Technology, Electronic Components, Technology and Materials, The Netherlands
[4]Máxima Medical Center, Veldhoven, The Netherlands

Keyword(s): biosignals – medical/clinical engineering

1. INTRODUCTION

Measuring the fetal heart rate (fHR) is a standard clinical tool to assess the fetal well-being during and before labour [1]. Typically, an ultrasound (US) transducer, operating in a pulsed wave Doppler mode, is used to non-invasively measure the periodic motion of the heart. A known problem of the US Doppler technique is its strong dependency on the relative position of the US transducer with respect to the fetal heart. When the fetal heart location (fHL) changes during measurements, either due to fetal movement within the uterus or due to a displacement of the US transducer on the maternal abdomen, fHR measurements often fail. Consequently, the clinical staff needs to manually reposition the US transducer to avoid long period of signal loss which can drastically compromise the clinical workflow. In this research, a flexible sensor matrix is designed which allows to measure the fHR over a large range of possible fHLs. Further, a method for dynamic combination of the receiving channels is proposed.

2. MATERIALS AND METHODS

A first prototype of a flexible ultrasound sensor matrix was realized by casting and curing a 1 mm thick layer of silicone (PDMS) into a mould. After curing at ~65 C°, 25 circular ceramic elements (PZT) were pressed into the layer at predefined positions. Each element was wired via 0.2 mm thick coaxial cables to an open ultrasound research platform (Vantage 256, Verasonics), which provides individual control over all elements. Eventually, a second layer of casted PDMS embeds the sensor elements for fixation and waterproofness.

The Doppler signals received in the individual transducer channels are traditionally combined by a simple summation method in order to generate one Doppler signal from which the fHR can be estimated. However, since the flexible sensor matrix increases the measurement volume many of the transducer elements are not directed towards the fetal heart and will therefore only measure noise. In order to reduce the contribution of channels measuring noise only, the power of each individual Doppler signal is computed. After that, the relative power in each element can be used to create dynamically changing weighting factors.

For validation of the flexible sensor matrix and the dynamic channel weighting (DCW) method a dedicated *in-vitro* setup was realized, which allows to mimic a beating-fetal heart at various fHLs.

3. RESULTS AND DISCUSSION

A new design of a flexible ultrasound sensor matrix is realized which allows to measure fHR independently of fHL. Using the *in-vitro* setup we showed a significant improvement of signal-to-noise (SNR) ratio of the Doppler signal using the DCW method compared to the traditional summation method. This improvement, along with the possibility to measure the fHR at varying fHLs without user interaction, represents a robust method for the clinical assessment of fetal well-being.

References

[1] Hammacher, K. et al. Fetal Heart Frequency and Perinatal Condition of the Fetus and Newborn. Gynecologic and Obstetric Investigation, 166,349–60, 1968.

ENDOMAGNET: MAGNETIC COMPRESSION ANASTOMOSIS BY THERAPEUTIC ENDOSCOPY

François Huberland[1*], Orianne Bastin[1], Nicolas Cauche[2], Cécilia Delattre[2], Ricardo Rio-Tinto[3], Jacques Devière[4], Alain Delchambre[1]

[1]Université Libre de Bruxelles, Biomed group, Belgium

[2]Brussels Medical Device Center, Belgium

[3]Faculdade de Medicina de Lisboa, Champalimaud Foundation, Portugal

[4]Hôpital Erasme, Service de Gastro-entérologie, Belgium

Keyword(s): medical/clinical engineering – Artificial organs and implants

1. INTRODUCTION

Interest for magnetic solutions used for endoscopy has grown in the past years [1]. Among those, magnetic pressure anastomosis has been already developed by different teams, but no solutions are yet available for physicians (illustrated in Figure 1). This solution enables leakage- and bleeding free procedure, without surgery. Reasons – not exhaustive – for that is the need for two endoscopes, the necessity of using a laparoscopic camera to secure the procedure, and the difficulty to have a wide opening compared to the device [1,3]. Our department is developing a new kind of magnetic solution, avoiding the problems described above.

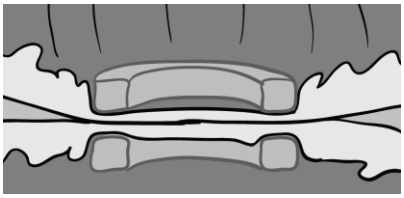

Figure 1: magnetic compression anastomosis. By compressing the tissues between both, magnets necrosis the tissue and create a hole.

2. MATERIALS AND METHODS

Our new devices aim to solve the three problems mentioned above (i.e. working with only one endoscope, no laparoscopy and having the capability of creating wider openings than the size of the magnet).

Two devices are under development:

- The first one intends to create wider anastomosis, based on a first small one. This device could be used to cure different pathologies, including oesophagal diverticulum or post-surgery complication, such as afferent loop syndrome post gastrectomy;
- The second one aims to create an anastomosis without surgery or laparoscopy. Similar solutions use stents, involving some problems with leakage, which would be solved thanks to magnets. This device could be used to cure different pathologies, including gastric-outlet obstruction (GOO) treatment, jejuno-jejunal bypass or duodenal switch.

3. RESULTS AND DISCUSSION

A fully working prototype of the first device has been developed and aim to be used in clinical studies by the end of 2018. A second device should be developed in the meantime. Such devices could also evolve to enable hybrid operation, involving surgeons and endoscopists. Indeed, the endoscopy could help for some part of the surgeries such as gastric bypass, were creating a leakage free gastro-jejunal anastomosis is a difficult challenge.

References

[1] Gottlieb, K.T. et al. Magnets in the GI tract. *Gastrointestinal Endoscopy,* 78(4), 561-567, 2013.

[2] Ryou, M. et al. Endoscopic intestinal bypass creation by using self-assembling magnets in a porcine model. *Gastrointestinal endoscopy,* 83(4), 821-825, 2016.

[3] Wall, J. et al. MAGNAMOSIS IV: magnetic compression anastomosis for minimally invasive colorectal surgery. *Endoscopy,* 45(08), 643-648, 2013.

Medical imaging

FUNCTIONAL CONNECTIVITY CHANGES DURING EPILEPTOGENESIS: A LONGITUDINAL RS-FMRI STUDY

Emma Christiaen[1*], Marie-Gabrielle Goossens[2], Benedicte Descamps[1], Paul Boon[2], Robrecht Raedt[2], Christian Vanhove[1]

[1]MEDISIP, Department of Electronics and Information Systems, Ghent University – IMEC, Belgium

[2]Laboratory for Clinical and Experimental Neurophysiology, Neurobiology and Neuropsychology (LCEN3), Department of Neurology, Ghent University, Belgium

Keyword(s): medical imaging

1. INTRODUCTION

Temporal lobe epilepsy (TLE) is the most common form of epilepsy in adults. Research has shown that abnormal functional brain networks could be involved in the development of epilepsy and its comorbidities [1]. Gaining more insight into these networks can be useful for the development of new therapies. Resting-state functional magnetic resonance imaging (rs-fMRI) can visualize changes in functional networks on a whole-brain level [2]. In this study, we aim to map changes in functional networks during epileptogenesis in the intraperitoneal kainic acid (IPKA) rat model for TLE using longitudinal resting-state fMRI and graph theory.

2. MATERIALS AND METHODS

Twenty-four adult male Sprague-Dawley rats (276 ± 15 g body weight) were used in this study. Seventeen animals were intraperitoneally injected with kainic acid (KA) according to the protocol of Hellier et al. [3] resulting in status epilepticus (SE). The other 7 animals were injected with saline and used as a control group. Rs-fMRI images were acquired before the KA injections and at 5 time points during the development of epilepsy. At each time point an anatomical image and three resting-state fMRI images were acquired on a 7T system, while the animals were anesthetized with medetomidine. The fMRI images were corrected for slice timing and motion, normalized, smoothed and band-pass filtered using SPM12. The Pearson correlation coefficient was calculated between the fMRI time series of 38 regions of interest (ROIs) and stored in a correlation matrix. After applying different thresholds to remove the weakest connections, several network measures were calculated using a graph theoretical network analysis toolbox (GRETNA), and plotted as a function of time to visualize how the properties of the functional networks change during epileptogenesis.

3. RESULTS AND DISCUSSION

In the IPKA rat model the correlation coefficients shift to smaller values during epileptogenesis, indicating that network connections progressively become weaker. Clustering coefficient and local efficiency decrease during epileptogenesis, indicating a decrease in segregation or local interconnectivity in the functional brain network. Characteristic path length increases and global efficiency decreases during epileptogenesis, indicating a decrease in integration or overall communication efficiency.

In the next phase of this study, EEG monitoring will be used to characterize the severity of epilepsy in these rats to investigate how changes in functional brain networks during epileptogenesis correlate with epilepsy severity.

References

[1] Chiang, S. & Haneef, Z. Graph theory findings in the pathophysiology of temporal lobe epilepsy. *Clin. Neurophysiol*. 125, 1295-1305, 2014.

[2] Hutchison, R. M., Mirsattari, S. M., Jones, C. K., Gati, J. S. & Leung, L. S. Functional Networks in the Anesthetized Rat Brain Revealed by Independent Component Analysis of Resting-State fMRI. *J. Neurophysiol*. 103(6), 3398-3406, 2010.

[3] Hellier, J. L., Patrylo, P. R., Buckmaster, P. S. & Dudek, F. E. Recurrent spontaneous motor seizures after repeated low-dose systemic treatment with kainate: assessment of a rat model of temporal lobe epilepsy. *Epilepsy Res.* 31, 73-84, 1998.

BRAIN TUMOUR CLASSIFICATION USING DEEP FEATURES FROM STRUCTURAL MRI

Milan Decuyper[1*], Roel Van Holen[1]

[1]Ghent University, Medical Image and Signal Processing (MEDISIP), Belgium

Keyword(s): medical imaging – medical/clinical engineering

1. INTRODUCTION

The ever-increasing amount of recorded medical imaging data contains valuable information that can improve brain tumour characterization. However, the rapid accumulation of large amounts of data becomes impossible for healthcare professionals to process. Artificial Intelligence can assist doctors in processing this data and leveraging it to efficiently obtain an accurate diagnosis. This study investigates the use of deep features, extracted from structural MRI images, for brain tumour classification. Deep features were extracted with a pre-trained convolutional neural network (CNN) similar to the approach introduced by Ahmed et al. [1]. However, the method is applied on a much larger database containing scans from different institutions. Moreover, both grade and survival time prediction performance has been studied.

2. MATERIALS AND METHODS

Data: In this work, the BRATS 2017 database was used containing T1, T2, T1 contrast enhanced (T1ce) and FLAIR MRI scans for 210 high-grade glioma (HGG) and 75 low-grade glioma (LGG) patients together with manual tumour segmentation labels [2,4]. For 163 HGG patients, survival data is available with 82 short-term (ST) and 81 long-term (LT) cases. Here, a survival time of 365 days was chosen as the classification criterion.

For each patient, the T1ce slice with the largest tumour contour was selected. Using the segmentation data, each selected slice was cropped to the size of the tumour and resized to 244x244 images as required by the CNN architecture used in this study.

Feature Extraction: The CNN used in this work is the VGG-F architecture [3]. It was pre-trained on the ImageNet dataset and provided by the MATLAB toolbox MatConvNet. The deep features were computed by forward propagating the tumour patches through the network and extracting the 4096-dimensional output of the second last fully connected layer.

Classification: A Random Forest classifier, preceded by a feature selection step based on symmetrical uncertainty, was used for classification. The number of selected features and trees was optimized and the performance was evaluated using 10-fold cross validation.

3. RESULTS AND DISCUSSION

The optimal number of selected features and trees was respectively 7 and 400 for survival prediction and 39 and 500 for grade prediction.

The system was able to distinguish ST from LT survival with an accuracy of 62% and LGG from HGG with an accuracy of 85%. The AUC scores were 66% and 92% respectively. Hence, this relatively simple approach already achieves a good performance in classifying brain tumour MRI images. The survival time prediction accuracy is lower than the 68% reported by Ahmed et al. However, they only validated the performance on a limited database of 22 HGG cases from one clinical center.

In this study, it was shown that a CNN, trained on images that are significantly different from medical scans, can effectively be used to obtain deep feature representations of MRI images.

References

[1] Ahmed K.B. et al. Fine-tuning convolutional deep features for MRI based brain tumor classification. *Proceedings of SPIE*, 10134, p. 101342E, 2017.

[2] Bakas S. et al. Advancing The Cancer Genome Atlas glioma MRI collections with expert segmentation labels and radiomic features. *Sci. Data*, 4, p. 170117, Sep. 2017.

[3] Chatfield K. et al. Return of the Devil in the Details: Delving Deep into Convolutional Nets. *BMVC*, 2014

[4] Menze B.H. et al. The Multimodal Brain Tumor Image Segmentation Benchmark (BRATS). *IEEE Transactions on Medical Imaging*, 34(10), pp. 1993–2024, Oct. 2015.

ULTRASOUND-BASED STRAIN MAPPING FOR QUANTITATIVE CHARACTERIZATION OF UTERINE ACTIVITY OUTSIDE PREGNANCY

Yizhou Huang[1*], Celine Blank[1,2,3], Federica Sammali[1], Nienke Petronella Maria Kuijsters[1,2], Benedictus Christiaan Schoot[2,3], Massimo Mischi[1]

[1]Department of Electrical Engineering (Signal Processing Systems), Eindhoven Technical University, Eindhoven, the Netherlands
[2]Department of Obstetrics and Gynecology, Catharina Hospital, Eindhoven, the Netherlands
[3]Department of Reproductive Medicine, University Hospital Ghent, Ghent, Belgium

Keyword(s): medical imaging

1. INTRODUCTION

Successful *In-Vitro* Fertilization (IVF) is achieved in 30% of the procedures only [1]. Implantation failure can possibly be caused by dysfunction of the uterine peristalsis (UP) [2]. The IVF success rate can therefore be improved by novel methods enabling objective and non-invasive characterization of UP. In this pilot study, strain mapping based on speckle tracking is applied on two-dimensional (2D) transvaginal ultrasound (TVUS) video loops to quantify UP outside pregnancy.

2. MATERIALS AND METHODS

Three healthy women, with a natural regular cycle, underwent 4-minute TVUS during active (before ovulation) and inactive (implantation) luteal phases of the menstrual cycle. Regions Of Interest (ROIs) were chosen to include the junctional zone close to the fundus. Strain mapping was applied to calculate and visualize strain variations in the ROIs. We considered contraction as negative strain and relaxation as positive strain. The obtained strain maps were rendered with suitable color maps; red color for relaxation and blue color for contraction.

3. RESULTS AND DISCUSSION

In each recording, 2D strain maps were generated along both longitudinal and transversal directions. Figure 1 shows an example of strain map in transversal direction for both active and inactive phases. We can clearly visualize the variations in strain around the junctional zone, revealing the propagation of the peristaltic movement.

The obtained results suggest the feasibility of accurate strain mapping in the uterus outside pregnancy. Extension of the method to 3D will overcome the current limitations with respect to out-of-plane motion. Future work will focus on the extraction of quantitative features in relation to contraction frequency and propagation. These features will then be evaluated in different phases of the menstrual cycle.

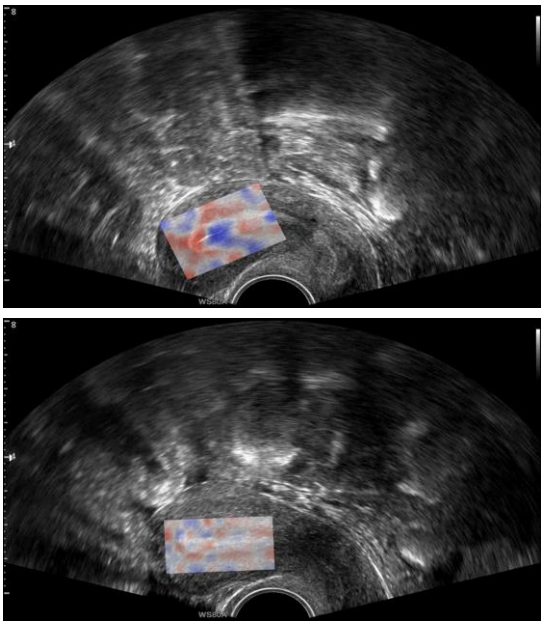

Figure 1: Strain map for the active phase (above) and the inactive phase (below)

References

[1] Nyboe Andersen, A. et al. Assisted reproductive technology in Europe, 2004: results generated from European registers by ESHRE. Human reproduction (Oxford, England), 23(4), 756-771, 2008.

[2] Fanchin, R. et al. Uterine contractions at the time of embryo transfer alter pregnancy rates after in-vitro fertilization. Human reproduction (Oxford, England), 13(7), 1968-1974, 1998.

4D-CT FOR MUSCULOSKELETAL APPLICATIONS: IMPACT OF SCAN PROTOCOL ON IMAGE REGISTRATION, MOTION ESTIMATION AND RADIATION DOSE

Benyameen Keelson[1*], Luca Buzzatti[2], Jildert Apperloo[2], Thierry Scheerlinck[3], Gert Van Gompel[3], Erik Cattrysse[2], Johan De Mey[3], Jef Vandemeulebroucke[1], Nico Buls[3]

[1]ETRO, Vrije Universiteit Brussels, Belgium,
[2]EXAN (KIMA), Vrije Universiteit Brussels, Belgium
[3]UZ Brussels, BEFY(RADI/ORTHO), Belgium

Keyword(s): medical imaging – medical/clinical engineering

1. INTRODUCTION

4D-CT is emerging as one of the techniques for studying joint motion [1]. Challenges however include reducing patient radiation exposure and the ability to automatically/semi automatically extract motion parameters. Image processing techniques such as registration and segmentation are potential tools for addressing the latter [2]. In this study, we investigated the impact of dynamic-CT acquisition parameters on registration of the ankle joint. Feasibility of detecting changes between the intact ankle and after ligament resection using registration was also investigated.

2. MATERIALS AND METHODS

Dynamic-CT acquisitions of two fresh frozen foot/ankle specimens were acquired during plantar-/dorsi-flexion on a 256-slice CT (GE Healthcare) with varying scan protocols. Using mutual information as similarity metric, the calcaneus and talus in the dynamic sequences were rigidly registered to a reference image dataset of the foot at rest. Dice Similarity Coefficient (DSC) and normalized mean absolute difference (nMAD) were computed as a measure for the registration. Scans were also performed with the intact ankle and after ligament cuts. Displacement of the calcaneus centroid served as a measure of kinematics.

3. RESULTS AND DISCUSSION

Registration quality (nMAD) depended on the tube rotation speed; faster temporal resolution performing significantly better ($p<0.003$). No kinematic differences were observed between high and low dose protocols. Reduced dose protocols had a radiation exposure that was three times lower. Plots of the centroid displacement against time showed differences of up to 2.02±0.41mm between the intact ankle and after ligament resections.

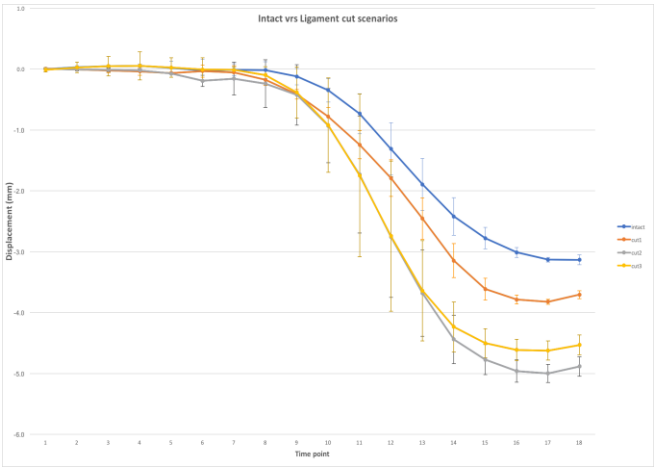

Figure 1. Plots of calcaneus centroid displacement as a function of time for the intact ankle(blue) and 3 different ligaments cut scenarios

In conclusion, a low dose protocol with fast tube rotation allowed to detect motion changes between the intact ankle and after ligament resection by means of image registration. This highlights the possibility to adopt 4D-CT to investigate MSK pathologies that may only be discernible during motion.

References

[1] Kwong, Y. et al. Four-dimensional computed tomography (4DCT): A review of the status and applications. Journal of medical imaging and radiation oncology, 59(5), 545-554, 2015.

[2] Miao, S. et al. Effective image registration for motion estimation in medical imaging, 2016.

ENDORULER: A REAL-TIME MEASUREMENT SYSTEM IN ENDOSCOPY

Maxime Pétré[1*], Benjamin Mertens[1], Alain Delchambre[1]

[1]Université libre de Bruxelles, Ecole polytechnique de Bruxelles, BEAMS Department, 50 Av. F.D. Roosevelt, 1050 Brussels, Belgium

Keyword(s): medical imaging – medical/clinical engineering

1. INTRODUCTION

Making measurements in endoscopy has been a problem for a long time since the current endoscopic cameras do not provide any precise information on distances and depth. This drawback can be compensated by the physician's experience [1] but it is a pain in many medical fields. In pneumology in particular it appears that the measurement of bronchus diameter is critical [2,3] before but also during an intervention. Tools such as CT-scan or MRI do not allow measuring during the intervention, and there is therefore a lack of necessary measurements. We have developed a device that can be used inside an endoscope to measure diameters and depth in real-time such as other existing device [4].

2. MATERIALS AND METHODS

Our device is using the structured light technique in order to get real-time information. A pattern is projected inside the human cavity. This pattern is recognized by the camera of the device and the position of each point is computed, offering a real-time measurement of the diameter of the cavity and the depth of each point. The Endoruler device is using a circular pattern which is very useful to measure circular ducts such as bronchus.

3. RESULTS AND DISCUSSION

A prototype of the device has been realized, compatible with endoscopes with channel of 2.8mm inner diameter. It has allowed performing tests on phantom organs. Experimental results showed an accuracy below the millimeter for diameters from up to 20mm.

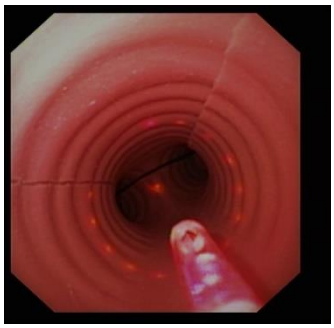

Figure 1: The Endoruler device is measuring the diameter of a phantom bronchus. The circular pattern (red dots) is visible.

Further improvements of the device will focus on the miniaturization

This will also expand the scope of possible applications to ENT, pediatric diseases (including pneumology and ENT); other fields where accurate measurements will improve diagnosis and therapeutic use of endoscopy.

References

[1] L. Cavallo, P. Cappabianca, and F. Esposito. Have 3d endoscopes succeeded in neurosurgery? *Acta neurochirurgica*, 156(8), 1631-1632, 2014.

[2] A. Begnaud, J.E. Connett, E.M. Harwood, M. A. Jantz, and H.J. Mehta. Measuring central airway obstruction, what do bronchoscopists do? *Annals of the American Thoracic Society*, 12(1), 85-90, 2015

[3] JP Williamson, AL James, MJ Phillips, DD Sampson, DR Hillman, and PR Eastwood. Quantifying tracheobronchial tree dimensions: methods, limitations and emerging techniques. *European Respiratory Journal,* 34(1), 42-55, 2009.

[4] M. Neitsch, I.-S. Horn, M. Hofer, A. Dietz and M. Fischer. Integrated Multipoint-Laser Endoscopic Airway Measurements by Transoral Approach. *BioMed Research International,* 2016.

PHARMACOKINETIC MODELING OF TARGETED MICROBUBBLES: APPLICATIONS IN ANGIOGENESIS IMAGING AND THERAPY MONITORING

S. Turco[1*], I. Tardy[2], P. Frinking[2], A.E. Kaffas[3], J. Zhou[3], J.K. Willman[3], H. Wijkstra[1], M. Mischi[1]

[1]Electrical Engineering, Eindhoven University of Technology, the Netherlands

[2]BRACCO SUISSE SA, Geneva, Switzerland

[3]Radiology, Stanford School of Medicine, United States

Keyword(s): medical imaging – modeling of physiological systems.

1. INTRODUCTION

The recognition of the key role of angiogenesis for cancer growth has opened new frontiers in oncology [1]. In cancer therapy, the development of novel drugs aimed at blocking angiogenic processes has spurred the need for imaging biomarkers able to assess and predict the response to therapy. In response, targeted contrast agents have been developed providing selective enhancement in areas of active angiogenesis by binding to specific molecules over-expressed in angiogenic tumor vasculature. In the context of ultrasound molecular imaging (USMI), the first and currently only clinical-translatable targeted ultrasound contrast agent (tUCA) is obtained from conventional UCA by decoration of the microbubble shell with ligands targeting the vascular endothelial growth receptor factor 2 (VEGFR2), over-expressed in several solid tumors [1]. Assessment of the level of binding has been adopted as an indirect way of quantifying angiogenesis. Semi-quantitatively, this is done by looking at the late-enhancement (LE) several minutes after injection, often in conjunction with the application of a high-pressure US burst to derive the differential targeted enhancement (dTE), i.e., the difference in the acoustic signal before and after the application of the high-pressure burst [1,2]. For quantitative assessment, we recently proposed pharmacokinetic modeling of the binding kinetics of tUCA by the first-pass binding model (FPB), enabling quantification of angiogenesis by estimation of the microbubble binding rate (K_b) [3]. Here, we show the feasibility of the method for angiogenesis imaging in 11 rat models of prostate cancer, and for therapy monitoring of colorectal cancer in 17 mice undergoing anti-angiogenic treatment.

2. MATERIALS AND METHODS

Time-intensity curves extracted at each pixel/voxel of USMI loops were fitted by the FPB model for estimation of the microbubble binding rate K_b. This was compared to semi-quantitative assessment by LE and dTE for: (i) angiogenesis imaging of prostate cancer by comparing parameter values in cancer and healthy regions of interest (ROIs) in 11 rats; (ii) anti-angiogenic therapy monitoring by comparing parameter values in responders, non-responders, and control mice at 5 time points during anti-angiogenic treatment.

3. RESULTS AND DISCUSSION

USMI parameters in healthy and tumor ROIs, obtained in 11 prostate-tumor bearing rats were significantly different (p-value<<0.01). In 17 colorectal cancer-bearing mice undergoing anti-angiogenic treatment, a significant decrease in the USMI parameters was observed only in the responder mice as early as one day after treatment initiation, especially by K_b (p-value <<0.01). In comparison, a significant increase in tumor volume only occurred 10 days after treatment (p-value<0.05). The results suggest the microbubble binding rate K_b to represent a promising quantitative biomarker of angiogenesis, enabling the distinction between healthy and cancer tissue, and the early prediction of the response to anti-antiangiogenic therapy.

References

[1] Abou-Elkacem, L. et al. Ultrasound molecular imaging: Moving toward clinical translation. *Eur J Radiol*, *84*(9), 1685-93, 2015.

[2] Frinking, P. et al. *Ultrasound in medicine & biology, 38*(8), 1460-69, 2012.

[3] Turco, S. *et al.* Quantitative ultrasound molecular imaging by modeling the binding kinetics of targeted contrast agent. *PMB*, 62(6), 2449, 2017.

SPARSITY-DRIVEN SUPER-RESOLUTION IN CLINICAL CONTRAST-ENHANCED ULTRASOUND

Ruud van Sloun[1*], Oren Solomon[2], Yonina Eldar[2], Hessel Wijkstra[3], Massimo Mischi[1]

[1]Eindhoven University of Technology, Biomedical Diagnostics Lab, Eindhoven, The Netherlands

[2]Technion – Israel Institute of Technology, Haifa, Israel

[3]Academical Medical Center University Hospital, Amsterdam, The Netherlands

Keyword(s): medical imaging

1. INTRODUCTION

Super-resolution (SR) ultrasound enables detailed assessment of the fine vascular network by pinpointing individual microbubbles (MBs), using ultrasound contrast agents (UCAs) [1]. The fidelity of SR images is determined by the density of localized MBs and their localization accuracy. To obtain high densities, one can evaluate extremely sparse subsets of MBs across thousands of frames by using a very low MB dose and imaging for a very long time, which is impractical for clinical routine. While ultrafast imaging somewhat alleviates this problem, long acquisition times are still required to enhance the full vascular bed. As a result, localization accuracy remains hampered by patient motion. The aim of this work is twofold. First, to attain a high MB localization accuracy on dense contrast-enhanced ultrasound (CEUS) data using a clinical dose of UCA and a widespread clinical scanner. Second, to retain a high resolution by motion compensation

2. MATERIALS AND METHODS

We performed transrectal imaging of the prostate using a Philips iU22 scanner (frame rate = 10 Hz). To analyze high-density frames in which many MBs are simultaneously present, we formulate the localization task as a sparsity-promoting convex optimization problem. Solving this corresponds to finding the sparse set of locations which, given the point spread function, adequately model the measured data. This process is repeated for a set of frames to accumulate a high number of localized MBs. Affine registration ensures that the locations are compensated for motion, and is performed using the pure-tissue fundamental mode images. The latter is facilitated by exploiting singular value decomposition to remove the MB signal components.

3. RESULTS AND DISCUSSION

Figure 1 shows the ability of the proposed method to resolve vessels beyond the diffraction limit from clinical prostate CEUS. The method can be applied effectively to achieve SR ultrasound imaging, facilitating a robust implementation in a clinical setting.

References

[1] Errico, C. *et al*. Ultrafast ultrasound localization microscopy for deep super-resolution vascular imaging. *Nature,* 527(7579), 499-502, 2015.

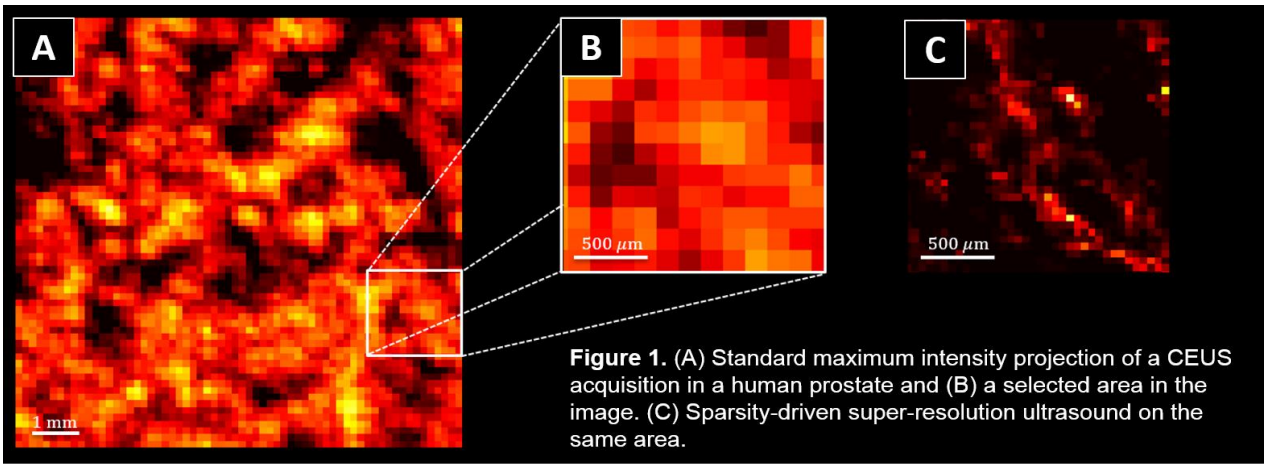

Figure 1. (A) Standard maximum intensity projection of a CEUS acquisition in a human prostate and (B) a selected area in the image. (C) Sparsity-driven super-resolution ultrasound on the same area.

ESTIMATION OF DISPERSION AND CONVECTION IN THREE-DIMENSIONAL CONTRAST ULTRASOUND IMAGING FOR PROSTATE CANCER LOCALIZATION

Rogier Wildeboer[1*], Ruud van Sloun[2], Stefan Schalk[1,2], Christophe Mannaerts[2], Hans van der Linden[3], Pintong Huang[4], Hessel Wijkstra[1,2], Massimo Mischi[1]

[1]Eindhoven University of Technology, Biomedical Diagnostics Labs, The Netherlands

[2]Academic Medical Centre University Hospital, Department of Urology, Amsterdam, The Netherlands

[3]Jeroen Bosch Hospital, DNA Laboratories / Dept of Pathology, 's-Hertogenbosch, The Netherlands

[4]Second Affiliated Hospital of Zeijiang University, Hangzhou, China

Keyword(s): medical imaging

1. INTRODUCTION

The extraction of dispersion- and convection-related parameters from Dynamic Contrast-Enhanced Ultrasound (DCE-US) recordings has shown promise to localize prostate cancer (PCa). In a two-dimensional (2D) approach, ultrasound-contrast-agent (UCA) dispersion and velocity were successfully used to characterize (micro)vasculature affected by PCa [1]. To this end, the UCA transport kinetics were modelled with strong assumptions on its directionality. In this work, we estimate convective dispersion (*D*) and velocity (*v*) of UCAs through the vascular network by directly solving the convective-dispersion equation in three dimensions (3D), without need for further assumptions. In addition, analysis of 3D recordings allows clinicians to examine the entire gland with a single UCA bolus injection. This approach thus enables us to provide independent 3D maps of *D* and *v* for the whole prostate.

2. MATERIALS AND METHODS

UCA dispersion and convection as defined in the convective-dispersion equation are considered for this method [2]. By establishing the concentration gradients of the data using Gaussian derivatives in space and time, the effect of noise is mitigated. Since we assume *D* and *v* to be locally constant, the convective-dispersion equation can then be successively solved by minimizing a least-squares problem in a moving spherical 3D kernel.

For the validation, we used 3D DCE-US loops of two minutes that were recorded at the Second Affiliated Hospital of Zhejiang University (Hangzhou, Zhejiang, China). Six patients referred for radical prostatectomy were selected for this feasibility study.

3. RESULTS AND DISCUSSION

For the entire prostate volume, we generated 3D maps of *D* and *v* and compared them to registered reconstructions of histopathology. Our preliminary results (Figure 1) show a good correlation between histopathologically-assessed malignancy and higher *v* and *D*. Although further validation and optimization is required, these results indicate the diagnostic potential of the obtained 3D maps of velocity and convective dispersion for the localization of PCa.

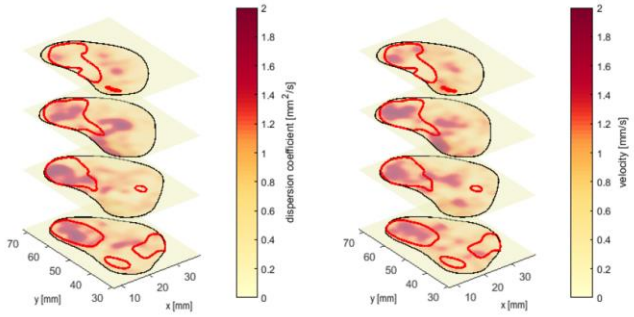

Figure | Example of multi-slice dispersion and velocity maps with PCa lesions delineated in red.

References

[1] van Sloun, R.J.G. et al. Ultrasound-contrast-agent dispersion and velocity imaging for prostate cancer localization. *Medical Image Analysis,* 35, 610-619, 2017

[2] Perl, W. and Chinard, F.P. A Convection-Diffusion Model of Indicator Transport through an Organ. *Circulation research*, *22*(2), 273-298, 1968.

Biomechanics

COMPUTATIONAL MODELING OF THE LYMPHATIC UPTAKE

Ghazal Adeli Koudehi[1*], Carlos Alejandro Silvera Delgado, Charlotte Debbaut[1], Christophe Casteleyn[2], Pieter Cornillie[2], Patrick Segers[1],

[1]IBiTech – bioMMeda Ghent University, Belgium
[2]POLITECNICO DI TORINO, Department of mechanical and Aerospace Engineering, Torino, Italy
[3]Faculty of Veterinary Medicine, Department of Morphology, Ghent University, Belgium

Keyword(s): medical/clinical engineering

1. INTRODUCTION

The lymphatic system consists of a unidirectional network of branches that, much alike the vascular system, expands throughout the body. Even though the lymphatic system plays crucial roles for maintaining a healthy human body, it has been rather neglected in comparison with the cardiovascular system. As a result, the mechanism of lymphatic uptake from the interstitium against the overall pressure gradient is still not fully understood. Looking at the lymphatic system at the microscale, we focus on the lymphatic capillaries (initial lymphatics). Initial lymphatics are blind-ended vessels mainly responsible for the uptake of fluid from the interstitium and introduction of lymph into the lymphatic system. These capillaries are made out of single layer endothelial cells that have a one-way valve-like function and do not permit the lymph to leak back into the interstitium after entering the lymphatic capillary. The purpose of this study was to computationally model the lymphatic uptake and the one-way mechanism of the primary valves in order to gain a better understanding of the factors that influence this phenomenon.

2. MATERIALS AND METHODS

COMSOL Multiphysics was used to perform the computational modeling. The 3D geometry includes 3 different domains being the inner volume of the lymph vessel, lymphatic wall and interstitium (Figure 1a). Lymph is the free fluid phase of the model which is only a section of a single initial lymphatic vessel. The lymphatic wall and interstitium were both considered as porous media. The one-way valve function of the wall was modeled by implementing a permeability that was dependent on the pressure gradient between the inlet and outlet. In other words, a positive pressure gradient drives the fluid into the lymph vessel, with the wall having high permeability. On the contrary, the wall permeability is reduced significantly to imitate the closing of the valves during negative pressure gradients. A sinusoidal pressure, ranging between 3 and -1 mmHg, was imposed at the inlet with a frequency of 0.4 Hz, to model the measured contracting frequency of lymphangions [1]. The pressure of the lymph was set to 0 mmHg as found in [2]. Periodic boundary conditions were imposed at the sides of the model.

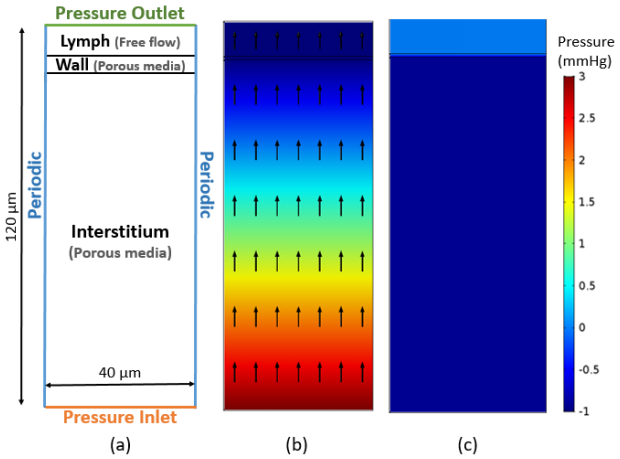

Figure 1: A 2D view of the 3D model (a) and pressure contours at max (b) and min (c) pressure inputs

3. RESULTS AND DISCUSSION

The results (Figure 1b and 1c). showed that the passage of fluid is not allowed when the pressure gradient is negative and that the lymph cannot return to the interstitium. However, these results are still at the preliminary stage since the geometry lacks the complexity of the actual lymphatics and it is merely a starting point for future studies.

References

[1] Dixon, J.B. et al. Lymph flow, shear stress, and lymphocyte velocity in rat mesenteric prenodal lymphatics. *Microcirculation*, 13(7), 597-610, 2006.

[2] Galie, P. et al. 2009. A two-dimensional computational model of lymph transport across primary lymphatic valves. *J Biomech Eng*, 131(11), p.111004, 2009.

CHARACTERIZATION OF BIOMECHANICAL PROPERTIES OF PORCINE MITRAL VALVE CHORDAE TENDINEAE

Shengda Chen[1*], Matthieu De Beule[2], Partick Segers[2], Xingshuang Ma[1]
[1]College of Bioengineering, Chongqing University, Chongqing 400044, China
[2]Institute Biomedical Technology, Ghent University, Ghent, Belgium

Keyword: biomechanics

1. INTRODUCTION

The mitral valve is a complex anatomical structure, including the annulus, anterior leaflet, posterior leaflet, papillary muscle, and chordae tendineae (chords). The mechanical properties of the chords play a key role in the normal functioning of the mitral valve: the chords help to maintain the opening and closing of the valve to achieve the whole body blood supply and resist blood backflow. Impaired chords may lead to mitral regurgitation or prolapse, which may subsequently lead to cardiac disabilities. In our study, we present an integrated experimental and computational constitutive study aiming at the characterization of the mechanical properties of the mitral valve chordae tendineae, and their mechanical interaction with the leaflets.

2. MATERIALS AND METHODS

Both the size and composition of porcine valves are similar to human's, so the porcine heart valve is often being used in experimental research [1]. A total of 58 fresh hearts from Rongchang pig were collected and perfused in saline at 4 ℃ in PBS buffer, and 55 of them were subjected to uniaxial mechanical tensile tests. We divided the chords into 7 kinds based on their insertion position and leaflets. added the marker point in the target area, and fixed the chordae onto an Instron 1000 uniaxial tensile test machine. Pre-load until the loading and unloading displacement curves were basically overlapped before tensile test. Using the mechanical sensor to record the stress change, the CCD camera synchronously collects the displacement image of the target area until the chordae breaks or slips. MATLAB codes were programmed for image recognition and the stress-strain curve reconstruction.

Histological analysis was performed to elucidate the association between the microstructure and the macro behavior of the chordae tendineae. The chords of 3 hearts were stained with picrosirius red for histologically observation by polarized light microscopy.

3. RESULTS AND DISCUSSION

The experimental results of the Green Strain - Cauchy stress curve are similar to those of the recent study [2] of human heart chords data. In general, the thicker chords have better ductility, the anterior leaflets chords are more ductile than the posterior ones.

With measurement of collagen fibril, the cycle of crimp was found smaller in thicker chordae than thinner chordae, which explained why the ductility of the thicker chordae is higher than thinner chordae. The Ogden nonlinear strain energy function provides the best fit of the experimental stress and strain data and the material parameters were obtained. This constitutive equation can simulate the biomechanical properties of the mitral valve chords, which can provide the basic theory for a subsequent dynamic simulation of the entire valve apparatus using the finite element method.

References

[1] Lam, J.H, Ranganathan, N., Wigle, E.D. Morphology of the human mitral valve. I. Chordae tendineae: a new classification. *Circulation,* 41(3), 449-458, 1970.

[2] Zuo, K., Pham, T., Li, K., Martin, C., He, Z. and Sun, W. et al. Characterization of biomechanical properties of aged human and ovine mitral valve chordae tendineae, *Journal of the mechanical behavior of biomedical materials,* 62, 607-618, 2016.

ROBOTIC MOTION SIMULATOR FOR TESTING ORTHOPEDIC AND PROSTHETIC DEVICES

Eveline De Raeve[1*], Tom Saey[1], Luiza Muraru[1], Veerle Creylman[1]
[1]Thomas More University of Applied Sciences, Mobilab, Belgium

Keyword(s): biomechanics

1. INTRODUCTION

During development process of new orthotic and prosthetic devices, mechanical tests and patient trials are common but have some disadvantages.

Patient trials are necessary in testing novel devices, but not always an option when safety is not yet guaranteed or when a controlled environment is desired.

Existing mechanical tests are controlled but rather simulate simplified conditions instead of complex movements that orthotics and prosthetics must sustain while being used by a patient [1]. Therefore, bench testing under realistic human kinematics and forces would be more appropriate in some cases.

We present a robotic motion simulator which mimics realistic human kinematics and forces aiming to combine advantages of mechanical tests and patient trials.

2. MATERIALS AND METHODS

As input for the robotic motion simulator a database was made. This database contains gait data of 70 healthy subjects during walking, 55 healthy subjects during running, each with 5 different types of running shoes and 10 amputees, each with 8 or 12 different prosthetic alignments. Ground reaction force and 3D movement of the foot, shank and upper leg were recorded simultaneously at 200Hz with a force plate (AMTI) and with a motion tracking system (Codamotion), respectively.

As a case study, a below-knee prosthesis with the same configuration as the one from patient measurement was connected to an artificial stump mounted on the end effector of an industrial robot with 6 degrees of freedom (KUKA). The movement of the subjects was recalculated to Euler angles to be used as kinematic input for this gait simulator. Ground reaction forces and motion were measured during unroll of a prosthetic foot with the robot.

3. RESULTS AND DISCUSSION

Figure 1 shows the movement of 3 markers in the sagittal plane and ground reaction force during the loading phase in human prosthetic walking and in robotic walking. It shows the similarity between human and robotic dynamics.

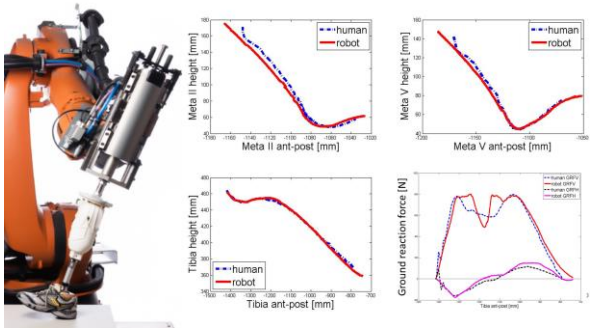

Figure 1: Comparison between robotic and human gait

Both kinematics and forces are adaptable in order to simulate new, complex, variable, individual or extreme motions and gait patterns. Recently we used the simulator to test durability and strength of insoles and additive manufactured prosthetic sockets, to determine influence of prosthetic alignment on stump pressure, to measure dynamic parameters of shoes and sports floors and to simulate the movement of an upper leg.

Using the robotic motion simulator described in this paper, different devices can be tested in a controlled environment, under realistic conditions and without risk for patients. Moreover, automated robot testing protocols can save time during development process of new products.

References

[1] Neo, L.D. et al. Principal structural testing of trans-tibial prosthetic assemblies: specimen preparation. *Prosthetic and Orthotic International,* 24, 241-245, 2000.

PROPAGATION-BASED PHASE-CONTRAST SYNCHROTRON IMAGING OF AORTIC DISSECTION IN MICE: FROM INDIVIDUAL ELASTIC LAMELLA TO 3D ANALYSIS

Gerlinde Logghe[1*], Bram Trachet[1,2], Lydia Aslanidou[2], Pablo Villaneuva-Perez[3], Julie De Backer[4], Nikolaos Stergiopulos[2], Marco Stampanoni[3], Hiroki Aoki[5], Patrick Segers[1]

[1]IBiTech – bioMMeda Ghent University, Belgium
[2]Ecole Polytechnique Federale de Lausanne, STI IBI-STI LHTC, Switzerland
[3]Paul Scherrer Institute, Switzerland. Pablo Villaneuva-Perez is now at CFEL, Germany
[4]Department of Cardiology and Center for Medical Genetics, Ghent University Hospital, Belgium
[5]Cardiovascular Research Institute, Kurume University, Japan

Keyword(s): biomechanics – medical/clinical engineering

1. INTRODUCTION

Over the past 3 years, we have made extensive use of PCXTM (phase contrast X-ray tomographic microscopy) for the ex-vivo imaging of excised murine aortas. We could demonstrate that, while being the most used aneurysm mouse model, ApoE$^{-/-}$ + Angiotensin II (AngII) mice actually develop medial tears that progress into aortic dissections (AD) [2]. The aim of this work was to use propagation-based phase-contrast synchrotron imaging rather than PCXTM, in order to obtain an improved isotropic resolution up to 1.6 µm. We applied this novel technique to qualitatively and quantitatively document the pathophysiology of lesion development, in 3D, in β-aminopropionitrile monofumarate (BAPN) + AngII mice, a known model of aortic dissection [1], with particular attention for events in the vicinity of aortic side branches and for the differences between ascending and abdominal aorta.

2. MATERIALS AND METHODS

Aortic samples from BAPN/AngII-infused (for 3, 7 and 14 days) and control mice were scanned with propagation-based phase-contrast synchrotron imaging at the Paul Sherrer Institute (Villigen, Switzerland) and analyzed for the progression of medial ruptures in 3D.

3. RESULTS AND DISCUSSION

A total of 268 lamellar ruptures were segmented, occurring both in control and treated animals. A steep increase in the number of ruptures was already noted after 3 days of BAPN/AngII-infusion, see Figure 1. Medial ruptures through all lamellar layers, leading to false channel formation and intramural hematoma, occurred only in the thoraco-abdominal aorta. All cases of interlamellar hematoma formation in the ascending aorta could be directly related to ruptures of the innermost lamellae.

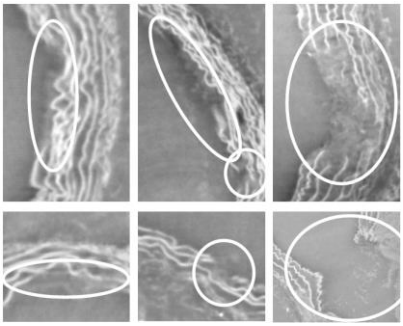

Figure 1: Representative images of ascending (top row) and abdominal aorta (bottom row) of day 3 (left), day 7 (middle) and day 14 (right) in BAPN/AngII infused mice.

We were able to show, in 3D, how small micro-ruptures seem to progress to large medial tears in BAPN/AngII mice, using phase-contrast imaging. This technique allows for ultra-high resolution, quantitative and qualitative analysis of rupture progress, 3D-analysis of the complete aorta, high contrast, and earlier detection of (micro-) ruptures.

References

[1] Kurihara, T. et al. Neutrophil-Derived Matrix Metalloproteinase 9 Triggers Acute Aortic Dissection. *Circulation*, 26, 3070–3080, 2012.

[2] Trachet, B. et al. Dissecting abdominal aortic aneurysm in Angiotensin II-infused mice: the importance of imaging. *Current Pharm Des*, 21(28), 4049-4060, 2015.

PREDICTION OF POST STENOTIC FLOW INSTABILITIES IN A PATIENT-SPECIFIC COMMON CAROTID ARTERY MODEL

Viviana Mancini[1*], Aslak Bergersen[2], Kristian Valen-Sendstad[2], Jan Vierendeels[3] , Patrick Segers[1]
[1]IBiTech – bioMMeda, Gent University, Belgium
[2]Scientific computing Simula Research Laboratory, Norway
[3] Department of Flow, Heat and Combustion Mechanics, Gent University, Belgium

Keyword(s): biomechanics – modeling of physiological systems

1. INTRODUCTION

The carotid arteries are the main vessels feeding the brain tissues and they are unfortunately very prone to develop atherosclerotic plaques close to the bifurcation. The growth of the plaques leads to the narrowing of the vessel, better known as stenosis. The severity of the stenoses in the internal carotid artery (ICA) strongly affects the blood flow towards the brain: a higher degree of stenosis leads to an higher risk of stroke. Furthermore, it is well known that the pulsatile nature of the flow in combination with narrowing of the lumen can cause post stenotic flow instabilities. The purpose of this study is to assess the relation between the turbulence level and the degree of stenosis in order to produce a turbulence-based threshold value for mild, severe and highly severe stenosis. This may open ways to diagnose stenosis severity from measurements of neck vibrations.

2. MATERIALS AND METHODS

CT images of a carotid bifurcation with 76% stenosis by area in the internal carotid artery [1] was manipulated by means of a VTK-based in-house code in order to reach 56%, 66%, 86% and 96% area stenosis. The five geometries were then meshed in 15M linear tetrahedral cells by means of VMTK. The flow split was set in order to mimic physiological values accordingly to the stenosis severity [2]. The pulsatile inflow was obtained by previously performed in-vitro tests with Reynolds number Re_{peak} of ~1400 with water. Simulations were performed by means of the 2nd order finite elements software Oasis [3].

3. RESULTS AND DISCUSSION

Results are shown for the 56%, 76% and 85% stenosis. The power spectral density (PSD) of the magnitude of the fluctuating velocity is plotted in logarithmic scale in Figure 2. The 56% stenosis behaves differently if compared with the more severe stenosis. It is not severe enough to induce a strong acceleration and then deceleration of the flow which hence behaves more like a laminar flow. The 76% stenosis is severe enough to trigger instabilities, but at a lower energy level than the 85% stenosis. These numerical results remain to be validated against hydraulic bench experiments and confirmed in vivo.

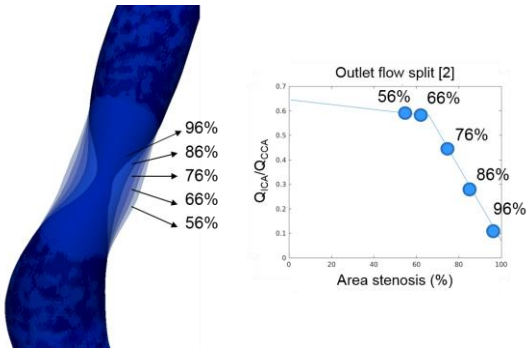

Figure 1: multiple degrees of stenosis and physiological flow split [2]

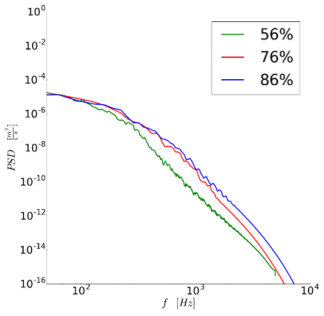

Figure 2: PSD of multiple degrees of stenosis

References

[1] *Iannaccone F. et al, Int J Arg Org*, 37:928-939, 2014.

[2] *Groen C. et al.,J Biomechs*, 43, 2332-2338, 2010

[3] *Mortensen M. et al, Comp Phys Comm*, 188, 177-188, 2015

LOW IMPLANTATION DEPTH DURING TAVR INCREASES THE PRESSURE EXERTED ON THE ATRIOVENTRICULAR CONDUCTION SYSTEM: A BIOMECHANICAL ANALYSIS

Giorgia Rocatello[1*], Nahid El Faquir[2], Patrick Segers[1], Matthieu De Beule[1,3], Peter Mortier[3], Peter de Jaegere[2]

[1]University of Gent, IBitech-bioMMeda, Belgium [* indicates presenting author]
[2]Erasmus MC, Department of Cardiology, The Netherlands
[3]FEops NV, Belgium

Keyword(s): medical imaging – medical/clinical engineering

1. INTRODUCTION

Low implantation depth has been associated with the occurrence of new conduction abnormalities after transcatheter aortic valve replacement (TAVR) [1]. However, the impact of implantation depth on the mechanical device-host interaction remains unclear [2].

We used patient-specific computer simulations to investigate the pressure that the stent frame exerts on the surrounding tissues in the vicinity of the atrioventricular (AV) conduction system, when implanted at different depths.

2. MATERIALS AND METHODS

Twenty patients who received an Evolut R (Medtronic, MN, USA) valve were included in this study. For each patient, a 3D aortic model was obtained from pre-operative CT images and a region of interest in the vicinity of the AV conduction system was defined. Finite-element computer simulations were used to virtually implant the device in a high, intermediate and low position. From each simulation the maximum contact pressure exerted by the frame on the region of interest and the relative area of contact were analyzed; differences were compared with the Friedman test.

3. RESULTS AND DISCUSSION

When implanted at a high implantation depth (3.3±1.3 mm) maximum contact pressure and relative area of contact were 0.28 [0.06-0.38] MPa and 8 [2-13]% respectively. For the intermediate implantation depth (7.2±1.3 mm), maximum contact pressure increased to 0.48 [0.35-0.73] MPa as did the relative contact area (29 [20-33]%). Highest values were obtained for the low implantation depth (10.9±1.3 mm), with maximal contact pressure 0.62 [0.52-0.69] MPa and relative contact area of 50 [39-55]%. Differences between the three different implantation depths were highly significant ($p<0.001$).

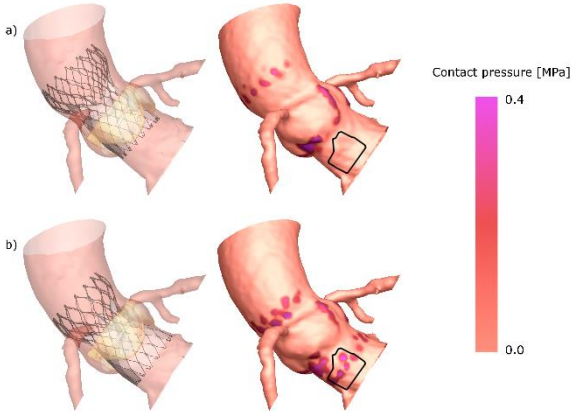

Figure 1. An example of high (a) and low (b) valve implantation in the same patient model and the obtained contact pressure (left). Region of interest in black.

We conclude that the maximum pressure generated by the valve frame on the tissue in the vicinity of the AV conduction system and the relative area of contact increase with the depth of valve implantation in TAVR.

References

[1] *Journal of Cardiovascular Computed Tomography*, 2017.

[2] Van der Boon R.M. et al. Trends in the occurrence of new conduction abnormalities after transcatheter aortic valve implantation. *Catheterization and Cardiovascular interventions, 85*(5), 2015.

BIOMECHANICS OF WAVE PROPAGATION THROUGH HYDROGELS MIMICKING SOFT BIOLOGICAL TISSUES

D. Tommasin[1*], A. Caenen[1], B. Verhegghe[1], S. E. Greenwald[2], P. Segers[1]

[1]IBiTech-bioMMeda, Ghent University, Ghent, Belgium
[2]Blizard Institute, Barts and The London School of Medicine and Dentistry, Queen Mary University of London, London, UK

Keyword: biomechanics

1. INTRODUCTION

The fluid dynamics inside arteries generate a pressure field which stretches and deforms the artery wall. It generates a perturbation which is transmitted as a combination of mechanical waves that propagates through the surrounding tissues (eg. muscles, fat and organs) to the skin surface. The skin vibrations are characterized by low amplitude displacement that can be detected with some optical techniques as laser Doppler vibrometry (LDV) [1]. The displacement patterns might be used to measure the local pulse wave velocity and reveal local flow anomalies (e.g. the presence of stenosis), [2]. Despite the promising potential of optical techniques for cardiovascular diagnosis, there are still some open questions: which is the correlation between the pressure signal in the lumen and the displacement at the skin level? How mechanical waves propagate and combine through soft tissues to the skin level? To better understand the physics of wave propagation, finite element models were implemented to simulate wave propagation through soft biological tissues. To allow for comparison with experiments, models were set up using properties of tissue mimicking hydrogel materials.

2. MATERIALS AND METHODS

Two geometries were considered: i) simplified artery geometry, ii) realistic bifurcation carotid artery. Both models were embedded (depth 10 mm) in an homogenous material. Two different hydrogels were considered: poly-vinyl alcohol (PVA) and chitosan hydrogel [4]. A travelling pressure impulse (velocity 4 m/s, amplitude 40 mmHg) was applied on the internal lumen. Simulations were performed in Abaqus/Explicit (Abaqus 14.1). Displacements on the lumen surface and on the external surface were observed.

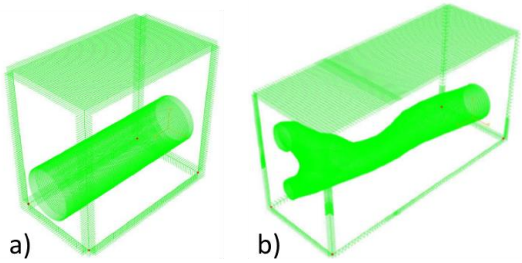

Figure 1. a) simplified artery model, b) carotid artery model

3. RESULTS AND DISCUSSION

Mechanical waves were generate by applying a pressure in the internal lumen and they propagated up to the external surface. A correlation was observed between the pulse propagating on the lumen surface and the external surface. Different propagation patterns were noticed for the PVA material (linear elastic material) and the hydrogel (hyperelastic material). This preliminary study confirms the possibility to reproduce the physics of wave propagation through two different tissue mimicking materials. Future developments will reproduce a more realistic pressure waveform and the effect of boundary conditions will be investigated.

References

[1] Li, Y. et al. On-chip laser Doppler vibrometer for arterial pulse wave velocity measurement. *Biomed Opt Express*, 4(7), 1229–1235, 2013.

[2] Seo, J.H. et al. A coupled flow-acoustic computational study of bruits from a modeled stenosed artery. *Med Biol Eng Comput*, 50(10), 1025–1035, 2012.

[3] Sasson, A. et al. Hyperelastic mechanical behavior of chitosan hydrogels for nucleus pulposus replacement—experimental testing and constitutive modeling. *J Mech Behav Biomed Mater*, 8, 143-153, 2012.

ESTIMATION OF GROUND REACTION FORCES BASED ON KINEMATIC DATA

Romain Van Hulle[1*], Cédric Schwartz[1], Olivier Brüls[1]
[1]University of Liège, Laboratory of Human Motion Analysis, Belgium

Keywords: biomechanics

1. INTRODUCTION

The inverse dynamics simulation of the musculoskeletal system is a common method to understand and analyse human motion.

To estimate the ground reaction forces, measuring them experimentally using force platforms is an accurate method. However, the number of steps is limited by the number of force platforms available in the lab. Several numerical methods have been proposed to estimate the ground reaction forces without force platforms, i.e. solely based on kinematic data.

The purpose of this work is to provide a more efficient method, using a simple rigid and unilaterally constrained model of the foot to compute the ground reaction forces. This way, the model of the foot is kept as simple as possible and does not require any data related with the compliance of the foot-ground contact.

2. MATERIALS AND METHODS

The equations of motion of a multibody system can be written, as [1]:

$$\begin{cases} \mathbf{M}(\mathbf{q})\ddot{\mathbf{q}}(t) + \mathbf{g}_{\mathbf{q}}^{\mathrm{T}}(\mathbf{q})\boldsymbol{\lambda} - \boldsymbol{f}(t) = \mathbf{0} & (1) \\ \mathbf{g}^{\boldsymbol{B}}(\mathbf{q}) = \mathbf{0} & (2) \\ \mathbf{0} \le \mathbf{g}^{\boldsymbol{U}} \perp \boldsymbol{\lambda}^{\boldsymbol{U}} \ge \mathbf{0} & (3) \end{cases}$$

where $\mathbf{g}^{\mathrm{T}} = [\mathbf{g}^{\boldsymbol{B},\mathrm{T}}, \mathbf{g}^{\boldsymbol{U},\mathrm{T}}]$ and $\boldsymbol{\lambda}^{\mathrm{T}} = [\boldsymbol{\lambda}^{\boldsymbol{B},\mathrm{T}}, \boldsymbol{\lambda}^{\boldsymbol{U},\mathrm{T}}]$, $\mathbf{M}(\mathbf{q})$ is the mass matrix, $\mathbf{q}$, $\dot{\mathbf{q}}$ and $\ddot{\mathbf{q}}$ are respectively the coordinates, velocities and accelerations vectors, $\mathbf{g}^{\boldsymbol{B}}(\mathbf{q})$ and $\mathbf{g}_{\mathbf{q}}^{\boldsymbol{B}}$ represent the bilateral kinematic constraints and the corresponding gradient, $\boldsymbol{\lambda}^{\boldsymbol{B}}$ denotes the Lagrange multipliers containing internal efforts, $\mathbf{g}^{\boldsymbol{U}}$ and $\mathbf{g}_{\mathbf{q}}^{\boldsymbol{U}}$ represent the unilateral constraints between the feet and the ground and their gradient, and $\boldsymbol{f}(t)$ is the vector of external forces, including the gravity forces.

The idea is to treat the contact forces as the set of unilateral reactions forces represented by the Lagrange multipliers $\boldsymbol{\lambda}^{\boldsymbol{U}}$.

Eq. (1) is the dynamic equilibrium of the system, and Eq. (2) represents the constraints which model the kinematic joints and the rigid body conditions. Eq. (3) represents a complementarity condition: if a constraint is activated ($\mathbf{g}_{\mathrm{j}}^{\boldsymbol{U}}(\mathbf{q}) = \mathbf{0}$) then the reaction force must be positive ($\boldsymbol{\lambda}_{\mathrm{j}}^{\boldsymbol{U}} \ge \mathbf{0}$). Conversely, if a gap is measured ($\mathbf{g}_{\mathrm{j}}^{\boldsymbol{U}}(\mathbf{q}) > \mathbf{0}$), the reaction force must be null ($\boldsymbol{\lambda}_{\mathrm{j}}^{\boldsymbol{U}} = \mathbf{0}$).

The values of $\mathbf{q}$, $\dot{\mathbf{q}}$ and $\ddot{\mathbf{q}}$ are measured experimentally during a gait test at the Laboratory of Human Motion Analysis of the University of Liège, using optoelectronic cameras and signal processing methods. Based on these kinematic data, our goal is to evaluate the unknown reaction forces $\boldsymbol{\lambda}$. The method relies on the identification of the active unilateral constraints and on a least-square inversion of Eq. (1).

3. RESULTS AND DISCUSSION

Figure 1 compares the vertical ground reaction forces obtained using the proposed approach and the force platforms.

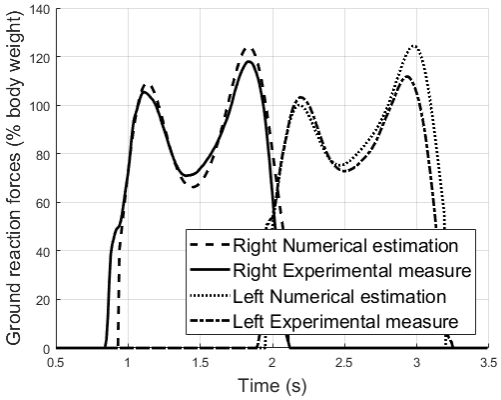

Fig. 1: Ground reaction forces

The proposed method produces encouraging results in a healthy gait test. Future work will address other cases, like pathological gait, running or jumps.

References

[1] Brüls, O. et al. *Computer methods in applied mechanics and engineering,* 281, 131-161, 2014.

Biosignals

A GAIT CYCLE PARTITIONING METHOD USING A FOOT-WORN ACCELEROMETER SYSTEM

Mohamed Boutaayamou[1,2*], Olivier Brüls[1], Vincent Denoël[1], Bénédicte Forthomme[1], Jean-Louis Croisier[1], Jacques G. Verly[2], Gaëtan Garraux[3], Cédric Schwartz[1]

[1]University of Liège (ULiège), Laboratory of Human Motion Analysis, Liège, Belgium
[2]ULiège, Department of Electrical Engineering and Computer Science, INTELSIG Laboratory, Belgium
[3]ULiège, GIGA - CRC In vivo Imaging, Liège, Belgium

Keywords: biosignals – biomechanics

1. INTRODUCTION

Accelerometer-based systems have been proposed as a reliable solution for the human gait analysis. Their hardware part has the advantage to include low-cost, small, and lightweight accelerometer units with generally low power consumption. Yet, in the context of accelerometer-based algorithms, there is a current unmet need of a validated extraction of temporal gait sub-phases, e.g., temporal sub-phases of the swing phase time, using recorded data solely from accelerometers. In this work, we describe a newly developed algorithm to extract durations of (1) left (L)/right (R) stride (Sr), stance (Sa), swing (Sw), and double support (DS) phases, and (2) L/R sub-phases that refine the L/R stance and swing phases, using our foot-worn accelerometer system [1]. The extracted temporal sub-phases include durations of (1) HS2TS (heel strike (HS) to toe strike (TS)), (2) TS2MS (TS to mid stance (MS)), (3) MS2TO (MS to toe-off (TO)), (4) TO2MHC (TO to maximum of heel clearance (MHC)), (5) MHC2MTC (MHC to maximum of toe clearance (MTC)), and (6) MTC2HS (MTC to HS).

2. MATERIALS AND METHODS

In order to accurately and precisely quantify the aforementioned gait phase/sub-phase durations, it is important to extract accurate and precise moments of gait events involved in the calculation of these phase/sub-phase durations. The proposed extraction algorithm uses distinctive and remarkable features on both longitudinal and antero-posterior accelerations of the heel and toe for each foot. Depending on the nature of these features, a suitable method is employed to accurately and precisely extract gait events of interest. We examine these gait phase/sub-phase durations for 6 walking speeds ranging from 0.70 to 1.39 m/s in treadmill walking of a healthy subject (female, 24 years old); and we estimate linear regression parameters of the mean values of these gait parameters during the 6 walking speeds.

3. RESULTS AND DISCUSSION

The results demonstrate that the proposed algorithm successfully quantifies 6 relevant sub-phase durations refining the gait cycle time for the 6 walking speeds. Most of the extracted gait phase/sub-phase durations change significantly with speed (Table 1). To the best of our knowledge, this is the first study that demonstrates the extraction, on a stride-by-stride basis, of the sub-phase durations of the swing phase for different walking speeds, using an ambulatory gait analysis system based solely on accelerometers. The extracted temporal gait phases/sub-phases could be relevant for characterizing, e.g., the progression of a neurological disease such as the Parkinson's disease, and for an early prediction of, e.g., elderly falls.

Table 1: Results of the linear regression of the mean values of the L/R phase/sub-phase percentages (of the L/R stride duration) for the 6 walking speeds.

Newly extracted phases/sub-phases (%)		*a* (%/(m/s))	*b* (%)	R^2
L/R Sr phases	Sa	−6.0	72.8	0.97
	Sw	6.1	27.1	0.98
	DS	−6.0	22.8	0.98
L/R Sa sub-phases	HS2TS	0.6	6.5	0.26
	TS2MS	−0.7	12.4	0.18
	MS2TO	−5.3	53.5	0.97
L/R Sw sub-phases	TO2MHC	1.2	3.4	0.98
	MHC2MTC	5.7	20.4	1.00
	MTC2HS	−0.8	3.2	0.50

- *a* and *b*: the linear regression parameters with: gait phase/sub-phase duration = *a* * walking speed + *b*);
- R^2: the coefficient of determination.

References

[1] Boutaayamou, M. et al. *Biomedical Engineering Systems and Technologies*, Springer, 2017.

DETECTING CARDIOVASCULAR COMORBIDITIES IN SLEEP APNEA PATIENTS USING SpO_2

Margot Deviaene[1,2*], Dries Testelmans[3], Pascal Borzée[3], Bertien Buyse[3], Sabine Van Huffel[1,2], Carolina Varon[1,2]

[1]KU Leuven, Department of Electrical Engineering (ESAT), STADIUS Center for Dynamical Systems, Signal Processing and Data Analytics, Leuven, Belgium
[2]Imec, Leuven, Belgium
[3]UZ Leuven, Department of Pneumology, Leuven, Belgium

Keyword(s): biosignals

1. INTRODUCTION

Studies have demonstrated the relationship between Obstructive Sleep Apnea Syndrome (OSAS) and cardiovascular comorbidities. It is even suggested that timely OSAS treatment can prevent the development of such comorbidities [1]. Hence, it is important to identify the patients with a high risk for cardiovascular comorbidities and prioritize their treatment. This study investigates if the blood oxygen saturation (SpO_2) signal could be used to assess the cardiovascular status of the patient.

2. MATERIALS AND METHODS

SpO_2 signals extracted from polysomnography recordings of 100 apnea patients at the sleep laboratory of the University Hospitals Leuven are analyzed. 50 patients with a known cardiovascular comorbidity are matched to patients without any comorbidity.

The analysis starts with an automatic detection of all oxygen desaturations. A total of 134 features are then extracted from these desaturations and the following resaturations. These contain simple time-domain, desaturation severity, statistical and quasi-periodicity features.

The features are used in a first step to build an apnea event classifier. Using the results of this classification, patient averaged features are computed for desaturations linked to apneic events or not. The most discriminative features to differentiate between patients with and without cardiovascular comorbidity are selected using a backwards wrapper after removing statistically non-significant and correlated features.

Based on these features an RBF least squares support vector machines classifier [2] is constructed which classifies patients as having a cardiovascular comorbidity or not.

3. RESULTS AND DISCUSSION

The Apnea event classifier yielded an accuracy of 80 % on the independent test set of 30 patients. The cardiac comorbidity feature selection resulted in the selection of seven features. Four of them were computed on apneic desaturations: the mean and median of the derivative, the median of the second order derivative of the SpO_2 desaturation and the deviation of the median SpO_2 value from the maximal value. The remaining features are the area under baseline, the deviation between the mean and maximum SpO2 value and the phase rectified signal averaging (PRSA) [3] slope computed on non-apneic desaturations. These features show an increase in desaturation severity and a delayed SpO_2 change after apneic events in apnea patients with a cardiovascular comorbidity. The cardiac comorbidity classification obtained an accuracy of 76.7 % on the independent test set of 30 patients. These findings suggest that the SpO_2 signal can have an added value in the assessment of cardiovascular comorbidities in sleep apnea patients.

References

[1] Marin, J.M. et al. Long-term cardiovascular outcomes in men with obstructive sleep apnoea-hypopnoea with or without treatment with continuous positive airway pressure: an observational study. *The Lancet, 365*(9464), 1046-1053, 2005.

[2] Suykens, J. et al. Least squares support vector machines. World Scientific, 2002.

[3] Bauer, A. et al. Phase-rectified signal averaging detects quasi-periodicities in non-stationary data. *Physica A: Statistical Mechanics and its Applications*, 364, 423-434, 2006.

THE EVOLUTION OF EEG COMPLEXITY DURING BRAIN MATURATION IN PRETERM INFANTS USING MULTISCALE ENTROPY

Ofelie De Wel[1,2*], Mario Lavanga[1,2], Alexander Caicedo[1,2], Anneleen Dereymaeker[3], Katrien Jansen[3,4], Gunnar Naulaers[3], Sabine Van Huffel[1,2]

[1]KU Leuven, Department of Electrical Engineering (ESAT), STADIUS Center for Dynamical Systems, Signal Processing and Data Analytics, Belgium
[2]imec, Leuven, Belgium
[3]University Hospitals Leuven, Department of Development and Regeneration, Neonatal Intensive Care Unit, Belgium
[4]University Hospitals Leuven, Department of Development and Regeneration, Child Neurology, Belgium

Keyword(s): biosignals – medical/clinical engineering

1. INTRODUCTION

Electroencephalography (EEG) is a valuable tool for continuous noninvasive brain monitoring of preterm infants in the neonatal intensive care unit. Automated extraction of features reflecting brain maturation from the neonatal EEG can assist clinicians in making a timely diagnosis and starting appropriate treatment [1]. This work investigates the evolution of EEG complexity during brain maturation in preterm infants. The underlying hypothesis is that the fast development of the preterm brain will result in more complex brain dynamics, which is in contrast with the reported loss of complexity during aging [2].

2. MATERIALS AND METHODS

The analysis is performed on a dataset consisting of 88 EEG recordings from 25 prematurely born infants, which were recorded at the University Hospitals of Leuven. The complexity of each channel of the neonatal EEG during quiet sleep is quantified using multiscale entropy (MSE), which assesses the degree of irregularity of a signal at multiple time scales. The MSE output, a curve of sample entropy in function of scale, is then used to derive the complexity index, which is the area under the MSE curve. Subsequently, a multiple linear regression model is adopted to describe the relationship between the EEG complexity indices and the postmenstrual age (PMA) of the infant.

3. RESULTS AND DISCUSSION

The multiple linear regression estimated the PMA of the infant with a root mean squared error of 2.04 weeks and an R^2 coefficient of 0.64. Moreover, correlation analysis revealed that there is a positive correlation between the complexity indices and the PMA, with an average Pearson's correlation coefficient of 0.73. This study has shown that the complexity of the EEG, measured using multiscale entropy, increases with maturation of the newborn. This finding indicates that the complexity index can be a highly useful feature to track brain maturation in preterm infants.

References

[1] O'Toole, J., Boylan, G. and Vanhatalo, S. Stevenson, N. Estimating functional brain maturity in very and extremely preterm neonates using automated analysis of the electroencephalogram. *Clinical Neurophysiology,* 127, 2910–2918, 2016.

[2] Janjarasjitt, S., Scher, M. and Loparo, K. Nonlinear dynamical analysis of the neonatal EEG time series: The relationship between neurodevelopment and complexity. *Clinical Neurophysiology,* 119, 822–836, 2008.

GEOMETRIC BROWNIAN MOTION (GBM) AS A PROMISING RANDOM PROCESS MODEL OF THE TIME EVOLUTION OF THE LEVEL OF DROWSINESS

Pouyan Ebrahimbabaie[1*], Jacques G. Verly[1]

[1]University of Liège, Department of Electrical Engineering and Computer Science, Liège, Belgium

Keyword(s): biosignals

1. INTRODUCTION

The drowsy state is an intermediate state between alert wakefulness and sleep. Drowsiness is a major cause of accidents in many areas of human activity, whether personal or professional. Transportation is probably the single most important source of drowsiness-related accidents; for example, one third of fatal accidents on highways in France are reported due to the driver falling asleep at the wheel.

It is thus critical to monitor the level of drowsiness (LoD) of a driver and to devise in-car safety systems that can help prevent drowsiness related accidents. This implies the development and use of drowsiness monitoring systems. We focus here on systems that monitor the physiological state of the subject, e.g. by using images of an eye. All systems that we know of can, at best, establish an LoD at the present time based on data obtained up to it. But, if the LoD at the present time reaches a critical level, it may be too late to save the life of a driver. Therefore, it is critical for drowsiness monitoring systems to also be able to predict future LoD values - at least a few (tens of) seconds ahead - based on data recorded up to the present time.

2. MATERIALS AND METHODS

The conventional approach to predict future values of a signal is to describe it via a model. Since the LoD evolves essentially in a random way, one must treat each real-life "LoD signal" as a realization of a random process (RP). The goal is then to identify RP models that are appropriate for such LoD signals. RP models that are often used in many applications are the AR, ARMA, and ARIMA models, where "AR" stands for "autoregressive", "MA" for "moving average", and "I" for "integrated". We examined the application of such models to LoD signals, and found that these signals could be properly modeled by AR(I)MA RP models. However, these models are quite computationally cumbersome to deal with, in part because their order is unknown and their parameters are unknown and numerous.

In the course of our investigation, we discovered that the RP process model called Geometric Brownian Motion (GBM) has excellent potential to model LoD signals and to predict future values thereof. This paper shows that real-life LoD signals are indeed well modeled by GBM RP models, or GBMs, for short.

3. RESULTS AND DISCUSSION

Our group has developed a system that continuously takes images of an eye, and automatically produces a validated LoD signal [1]. Using this system, we obtained LoD signals from 17 healthy subjects who performed psychomotor vigilance tasks (PVTs) and 13 subjects who performed driving tests in a fixed-base, high-fidelity driving simulator at 3 different states of sleep deprivation. For each of the above (13 + 17) x 3 = 90 LoD signals, we established whether or not GBM was a good model choice by applying the conventionally applied procedure of verifying that the logarithms of the ratios of successive values are normally distributed and uncorrelated in time.

We found out that each of the above 90 LoD signals passed the above statistical tests, meaning that GBM is a good model choice for each of these 90 signals.

References

[1] François, C. et al. Tests of a new drowsiness characterization and monitoring system based on ocular parameters. *International journal of environmental research and public health*, *13*(2), 174, 2016.

EFFECTIVENESS OF GEOMETRIC BROWNIAN MOTION (GBM) RANDOM PROCESS MODEL FOR MODELLING THE PRECLOS SIGNALS OF NARCOLEPTIC SUBJECTS

Pouyan Ebrahimbabaie[1*], Sofia Kermi[1], Jacques G. Verly[1]

[1]University of Liège, Department of Electrical Engineering and Computer Science, Liège, Belgium

Keyword(s): biosignals

1. INTRODUCTION

The Mayo Clinic defines narcolepsy as a chronic sleep disorder characterized by overwhelming daytime drowsiness and sudden attacks of sleep. It is a rare sleep disorder (1 in every 2,000 people in the US) and its exact cause is unknown. There are two types of narcolepsy: type 1, accompanied by a sudden loss of muscle tone (cataplexy) that leads to weakness & loss of muscle control, and type 2, or narcolepsy without cataplexy. Narcolepsy can be difficult to diagnose since its main symptoms (i.e. fatigue and excessive daytime sleepiness) fall into the broad categories of sleep disorders. Therefore, misdiagnosis is commonplace. The most common misdiagnoses are depression (almost 1/3 of patients), insomnia, & sleep apnea.

Here, we attempt to shed some light on the time evolution of an informative ocular parameter called PERCLOS (PERcentage CLOSure) in narcoleptic subjects without cataplexy. The PERCLOS for one eye and a given time window of duration T seconds (typically 20) is the total time where the eye is closed more than, say, 80% with respect to some reference maximum opening, divided by the window duration.

Our hypothesis is that the analysis of the time evolution of "PERCLOS signals" could ultimately lead to new diagnostic tools. Additionally, an understanding of this evolution would enable the design and construction of drowsiness monitoring systems specifically tailored to narcoleptic subjects, allowing them to drive more safely and to get, or recover, a driving license.

2. MATERIALS AND METHODS

Given that the motion of the eyelids, governed by complex physiological phenomena, has a significant random part, the evolution of the PERCLOS is inherently random. Therefore, one must treat each real-life "PERCLOS signal" as a realization of a random process (RP).

A number of our recent studies have focused on identifying RP models that are appropriate for the time evolution of the level of drowsiness and PERCLOS signals in healthy subjects. In a previous publication, we showed that the PERCLOS of healthy subjects evolves in time according to a particular RP model called Geometric Brownian Motion (GBM) [1]. In this study, we seek to determine whether or not the "PERCLOS signals" of narcoleptic subjects also evolve in time according to a GBM RP.

3. RESULTS AND DISCUSSION

Using a glasses-based system imaging one eye that was developed in our group, we obtained 4x2 + 3x2 = 14 PERCLOS signals from 4 narcoleptic subjects who performed psychomotor vigilance tasks (PVTs) and driving test in a fixed-base, high-fidelity driving simulator.

We subjected all 14 PERCLOS signals to required statistical tests, to check whether or not they evolve in time according to a GBM and concluded that all of them could be well modeled by a GBM RP model.

The preliminary results described here suggest that, similar to a healthy subject, the PERCLOS of a narcoleptic patient evolves in time according to a GBM. However, the hypothesis that most ERCLOS signals in most narcoleptic subjects evolve in time according to GBM needs further support and investigation.

References

[1] Ebrahimbabaie, P. and Verly, J. Geometric Brownian Motion (GBM) random process model appears to be an excellent choice for modeling realizations of PERCLOS signals. *World Sleep, Prague, Czech Republic*, 7-12 October 2017.

IDENTIFYING NEUROVASCULAR COUPLING IN BRAIN NETWORKS THROUGH STRUCTURED MATRIX-TENSOR FACTORIZATION OF EEG-FMRI DATA

Simon Van Eyndhoven[1,2*], Borbála Hunyadi[1,2], Lieven De Lathauwer[1,3], Sabine Van Huffel[1,2]

[1]KU Leuven, Department of Electrical Engineering (ESAT), STADIUS Center for Dynamical Systems, Signal Processing and Data Analytics, Leuven, Belgium

[2]imec, Leuven, Belgium

[3]KU Leuven Kulak, Group Science, Engineering and Technology, Kortrijk, Belgium

Keyword(s): biosignals

1. INTRODUCTION

In the field of neuroimaging and brain mapping, the combined use of electroencephalography (EEG) and functional magnetic resonance imaging (fMRI) is a promising approach to analyze cognitive or pathological neural activity, since it exploits both the complementary high temporal resolution from EEG and the excellent spatial resolution from fMRI. In order to fuse the heterogeneous data streams, containing contributions from many neural processes and/or nuisance components, the interrelationship between electrophysiological activity (captured by EEG) and corresponding hemodynamic fluctuations (captured by fMRI) should be known. This is known as neurovascular coupling, and is often modelled by a standard hemodynamic response function (HRF). However, the coupling displays a significant variability over people, brain areas and over time, and hence, misspecification of the HRF leads to biased estimates of activity (e.g. wrong localization in the brain) [1]. A chicken-and-egg problem arises, because knowledge of the HRF is needed for accurate mapping of the neural sources in the brain, but the sources are themselves needed to estimate the HRF. We aim to tackle this issue by proposing a novel blind source separation (BSS) approach to extract sources of neural activity from the EEG and fMRI recordings, in which we account for (a priori unknown) neurovascular coupling, which is simultaneously co-estimated.

2. MATERIALS AND METHODS

To unravel the data into the different underlying sources of activity, we developed a matrix-tensor factorization, which simultaneously decomposes an fMRI dataset (time samples $\times$ voxels) and an EEG spectrogram (time samples $\times$ electrodes $\times$ frequencies), yielding temporal, spatial, and spectral signatures for every source [2]. The effect of neurovascular coupling is captured by imposing a Toeplitz-structure on one of the factors. We simulated several neural sources and HRFs, which were combined to yield corresponding EEG and fMRI observations, and added different types of noise with varying signal-to-noise ratio. Hereafter, we applied the matrix-tensor factorization and verified whether it could accurately reconstruct the original sources from the noisy data.

3. RESULTS AND DISCUSSION

The neural sources that underlie the data are more accurately estimated when accounting for the variability in neurovascular coupling, as compared to using a standard HRF. The performance is especially high at lower levels of white Gaussian noise. In more realistic conditions of temporally or spatially correlated noise, a better localization of sources is possible. The HRF itself can generally be reconstructed quite well, if the algorithm is properly initialized.

These results demonstrate that accounting for HRF variability has a beneficial effect on the estimation of spatial, temporal, and spectral characteristics of neural sources from combined EEG-fMRI measurements. For this purpose, we have introduced a generic matrix-tensor factorization, which can be used to effectively identify patterns of neural activity.

References

[1] Lindquist, M.A. et al. Modeling the hemodynamic response function in fMRI: efficiency, bias and mis-modeling. *Neuroimage*, 45(1), S187-S198, 2009.

[2] Van Eyndhoven, Simon, et al. *Proc. of the 25th European Signal Processing Conference*. (2017): pp. 26-30

A METHOD FOR SLEEP APNEA HYPOPNEA SYNDROME CLASSIFICATION IN SPO_2 SIGNALS

John F. Morales[1*], Carolina Varon[1,2], Margot Deviaene[1,2], Pascal Borzee[3], Dries Testelmans[3], Bertien Buyse[3], Sabine van Huffel[1,2]

[1] KU Leuven, Stadius Center for Dynamical Systems, Signal Processing and Data Analytics, Belgium

[2]IMEC, Leuven, Belgium

[3] UZ Leuven, Department of Pneumology, Leuven, Belgium

Keyword(s): biosignals

1. INTRODUCTION

Sleep Apnea Hypopnea Syndrome (SAHS) is a condition characterized by repetitive airflow reductions (hypopneas) or cessations (apneas) during sleep. The current standard test for diagnosing SAHS is the polysomnography (PSG). This test is known to be expensive and uncomfortable. Hence, the development of home monitoring techniques is desirable. This work proposes a method based on SpO_2. This signal is highly unstable in patients with SAHS presenting abnormal slow desaturations and fast resaturations. Normal patients, on the other hand, have almost constant SpO_2 levels. The signals acquired during PSG are used to calculate the Apnea Hypopnea Index (AHI), which is defined as the average number of apneic or hypopneic events in one hour of sleep, and allows to classify the SAHS as normal (AHI < 5), mild (5 ≤ AHI < 15), moderate (15 ≤ AHI < 30) or severe (AHI ≥ 30). This study uses features extracted from the phase space reconstruction of the wavelet decomposition of SpO_2 signals to classify patients with different values of AHI.

2. MATERIALS AND METHODS

Polysomnographic studies from 79 subjects recorded at the University Hospital Leuven in Belgium were used. The dataset includes 47 men and 32 women with an average age of 49 ± 11.7 years, and a mean Body Mass Index (BMI) of 27.57 ± 4.42 kg/m^2. 31 patients had severe SAHS, 17 moderate SAHS, 17 mild SAHS, and 14 were normal. The AHI was calculated using the AASM 2012 rules [1]. Only the SpO_2 signals were used in this study. First, the wavelet decomposition of the SpO_2 signal was calculated in 7 levels with the Haar wavelet. After that, the Phase Space reconstruction of each of the wavelet components was built using the embedding dimension method. From the phase spaces, the area spanned by the cloud of points was calculated using the convex hull algorithm. Finally, the calculated areas were used as features to feed a K_{nn} and a LS-SVM [2] classifiers considering a patient with an AHI lower than 5 as normal.

3. RESULTS AND DISCUSSION

Table I shows the obtained results. The accuracies, specificities and sensitivities suggest that the extracted features can discriminate between the two groups. The performance of the K_{nn} is better. However, the performance of this algorithm is not trustworthy when the problem is unbalanced, as in this dataset where only 17.7% of the subjects have an AHI lower than 5. LS-SVM shows a poorer performance but, with a smarter parametrization of the classifier, the results can be improved. The proposed method is not computationally expensive, is easy to implement, easy to understand, and only a few features derived from a single signal are used. These factors are important in the development of methods for home monitoring of SAHS.

TABLE I

RESULTS OF THE TWO CLASSIFICATION METHODS WITH THE LEAVE-ONE-OUT VALIDATION

Leave-One-Out validation			
Algorithm	**Specificity**	**Sensitivity**	**Accuracy**
Knn	78.57%	96.92%	93.67%
LS-SVM	64.29%	93.85%	88.61%

References

[1] Berry R.B. et al. The AASM manual for the scoring of sleep and associated events. *Rules, Terminology and Technical Specifications, Darien, Illinois, American Academy of Sleep Medicine*, 2012.

[2] Suykens J.A. et al. Least squares support vector machine classifiers. *Neural processing letters*, 9(3), 293-300, 1999.

ASSESSMENT OF THE EFFECTS OF PROPOFOL ON THE CEREBRAL HEMODYNAMIC REGULATION MECHANISMS OF PREMATURE NEONATES USING GRAPHS

Dries Hendrikx[1*], Alexander Caicedo[1,2], Liesbeth Thewissen[3,4], Anne Smits[5], Gunnar Naulaers[3,4], Karel Allegaert[3,6,7], Sabine Van Huffel[1,2]

[1]Department of Electrical Engineering (ESAT), STADIUS, KU Leuven, Belgium
[2]imec, Leuven, Belgium
[3]Department of Development and Regeneration, KU Leuven, Belgium
[4]Department of Neonatology, UZ Leuven, Belgium
[5]Department of Pediatrics, UZ Leuven, Belgium
[6]Department of Pediatric Surgery and Intensive Care, Erasmus MC-Sophia Children's Hospital, Rotterdam, The Netherlands
[7]Department of Neonatology, Erasmus MC-Sophia Children's Hospital, Rotterdam, The Netherlands

Keyword(s): biosignals

1. INTRODUCTION

Sedation of premature neonates with propofol is frequently associated with a pronounced decrease in mean arterial blood pressure (MABP), often leading to hypotension [1]. The decrease in MABP is generally attributed to the vasodilatory action of propofol with a limited baroreceptor reflex. Guidelines on propofol dosing, particularly in highly vulnerable neonates, are highly variable [2]. In addition, precise physiologic responses to propofol remain unclear and are characterized by a great inter-individual variability [3].

2. MATERIALS AND METHODS

Concomitant measurements of heart rate (HR), MABP, arterial oxygen saturation (SaO_2), regional cerebral oxygen saturation ($rScO_2$) measured by means of near-infrared spectroscopy (NIRS), and EEG were performed in 22 neonates undergoing INSURE (intubation, surfactant, extubation). All signals were recorded from at least 5 minutes before propofol administration and lasted up to 12 hours after propofol was given.

The common dynamics between the different signals were analyzed using graphs. The graph model consists of five nodes, corresponding to the signal modalities of the multimodal data set and ten edges, since an edge is present between each of the nodes. The edge weights indicate the strength in dynamical coupling between two modalities and are calculated using the RBF kernel function.

3. RESULTS AND DISCUSSION

Propofol induces a decrease in common dynamics between the different signals of the multimodal dataset under study. Overall, this effect is observed to be restored in 90 minutes, and is mainly determined by the recovery of EEG dynamics, which were observed to recover much slower compared to the other modalities. In addition, the decoupling effect is more pronounced with increasing postmenstrual age (PMA) and propofol dose.

References

[1] Welzing L., Kribs A., Eifinger F., Huenseler C., Oberthuer A., and Roth B., Propofol as an induction agent for endotracheal intubation can cause significant arterial hypotension in preterm neonates. *Paediatr. Anaesth.*, 20, 605-611, 2010.

[2] Simons S. H. P., van der Lee R., Reiss I. K. M., and van Weissenbruch M. M., Clinical evaluation of propofol as sedative for endotracheal intubation in neonates. *Acta. Paediatr.*, 102, 487-492, 2013.

[3] Allegaert K., Peeters M. Y., Verbesselt R., Tibboel D., Naulaers G., de Hoon J. N., and Knibbe C. A., Inter-individual variability in propofol pharmacokinetics in preterm and term neonates. *Br. J. Anaesth.*, 99(6), 864-870, 2007.

UNSUPERVISED LEARNING FOR MENTAL STRESS DETECTION - EXPLORATION OF SELF-ORGANIZING MAPS

Dorien Huysmans[1,2*], Elena Smets[2], Walter De Raedt[2], Chris Van Hoof[2,3], Katleen Bogaerts[4,5], Ilse Van Diest[5], Denis Helic[6]

[1]KU Leuven, Stadius Center for Dynamical Systems, Signal Processing and Data Analytics, Belgium

[2]imec, Belgium

[3]imec, Holst Centre, The Netherlands

[4]REVAL - Rehabilitation Research Center, Hasselt University, Belgium

[5]Research Group on Health Psychology, Department of Psychology, KU Leuven, Belgium

[6]Knowledge Technologies Institute, Graz University of Technology, Austria

Keyword(s): biosignals – modeling of physiological systems

1. INTRODUCTION

One of the major challenges in the field of ambulant stress detection lies in the model validation. Commonly, different types of questionnaires are used to record perceived stress levels. These only capture stress levels at discrete moments in time and are prone to subjective inaccuracies.

Although, many studies have already reported such issues, a solution for these difficulties is still lacking.

This paper explores the potential of unsupervised learning with Self-Organizing Maps (SOM) for stress detection. In unsupervised learning settings, the labels from perceived stress levels are not needed anymore. The SOM in particular has been successfully applied in many other fields such as brain computer interfaces and geophysics.

The algorithmic pipeline only relies on the recorded physiological signals and no expert observations are required for marking stress and relax states within the SOM.

The findings will enhance our understanding of the link between physiological signals and stressors and may advise further strategies for stress detection in ambulatory settings.

2. MATERIALS AND METHODS

The data set consisted of a group of 12 test subjects. They all reported stress-related complaints, suffering from chronic stress, but were not diagnosed with any clinical disorder (e.g. depression or burnout).

First, a controlled stress experiment was conducted during which relax and stress-inducing phases were alternated. The skin conductance (SC) and electrocardiogram (ECG) of test subjects were recorded. Then, the structure of the SOM was built based on a training set of SC response and heart rate variability features. A Gaussian Mixture Model was used to cluster regions of the SOM with similar characteristics. Finally, by comparison of features values within each cluster, two clusters could be associated to either relax phases or stress phases.

3. RESULTS AND DISCUSSION

A classification performance of 79.0% (±5.16) was reached with a sensitivity of 75.6% (±11.2). Smets et al. [1] had a similar experimental setup and reported a maximum performance rate for non-personalized models of 82.7% using supervised support vector machines. Similar features for ECG and SC were applied, with additional temperature and respiration features. As performances are comparable and unsupervised techniques are generally harder to apply, the potential of SOM for stress detection exists.

In the future, the goal is to transfer these first initial results from a controlled laboratory setting to an ambulant environment.

References

[1] Smets, E. et al. Comparison of Machine Learning Techniques for Psychophysiological Stress Detection. *Springer International Publishing*, 13–22, 2016.

AN EEG MATURATION STUDY BASED ON MULTIFRACTALITY IN PRETERM NEONATES

Mario Lavanga[1,2*], Ofelie De Wel[1,2], Alexander Caicedo Dorado[1,2], Katrien Jansen[3], Anneleen Dereymaeker[3], Gunnar Naulears[3], Sabine Van Huffel[1,2]

[1]KU Leuven, STADIUS, Center for Dynamical Systems, Signal Processing and Data Analytics, Belgium

[2]imec, Belgium

[3] UZ Leuven, Department of Development and Regeneration, Neonatal Intensive Care Unit, Belgium

Keyword(s): biosignals – medical/clinical engineering

1. INTRODUCTION

Premature infant's EEG is characterized by high levels of discontinuity, which are expected to decrease with the brain development. In the literature, multiple parameters to assess electrocortical changes based on the EEG waveform have been investigated. In the present study, we propose the multifractal formalism to describe the EEG-based brain development. According to Wendt [1], the different regularities and geometrical properties of time series can be summarized via the Singularity Spectrum (SS). Roughly speaking, signals can be described by different degrees of multifractality based on the width of the singularity spectrum (SS): the narrower the spectrum, the lower the multifractality and vice versa. The underlying hypothesis is that the discontinuity is characterized by high degree of multifractality, which should decrease with neurodevelopment of the neonate. Therefore, the aims of the study were to provide insights of EEG changes from a chaotic point of view and to predict the age of the patient.

2. MATERIALS AND METHODS

EEG data from 25 healthy preterm infants were recorded at least twice during their stay in the NICU. The data were recorded with the 10-20 international system with fs = 250 Hz. The post-menstrual age (PMA) of all recordings range from 27 to 42 weeks, with a total number of 88 recordings. The SS can be estimated via wavelet leaders and its morphology can be characterized by the most frequent Hurst exponent (C1) and the width of SS, which can be expressed by either |C2| or the difference between the maximum and minimum Hurst exponents (ΔH) [1]. Data were uniformly segmented and the duet C1 and |C2| as well as ΔH were extracted in each window. The features were subsequently averaged throughout the quiet sleep period according to clinicians' labelling. In order to predict the infants' PMA, a linear regression model with the computed attributes was estimated and assessed via the coefficient of determination (R2) and the root mean squared error (RMSE).

3. RESULTS AND DISCUSSION

The results show that the multifractal features decrease with maturation. Considering only channel T3 and F1, the Pearson correlation coefficient of C1, |C2| and ΔH with PMA were respectively -61%, -42%, -55%. The linear model can predict the recording PMA with RMSE of 2.67, 3.04, 2.73 weeks and R^2 of 0.50, 0.34, 0.52 respectively. These findings suggest that the reduction of discontinuity in premature EEG can be explained by a decrease in the level of multifractality in the EEG. Furthermore, the signal has reduction in the parameter C1, which underlies a shift towards a less predictable and less regular pattern. Eventually, the multifractal features can predict the age of the infant with an accuracy comparable to the literature.

References

[1] Wendt, H., Abry, P. and Jaffard, S. Bootstrap for Multifractal Analysis. *IEEE Signal Processing Magazine,* 24(4), 38-48, 2007.

IRREGULAR HEARTBEAT CLASSIFICATION USING MULTISCALE TENSOR ANALYSIS

Sibasankar Padhy[1*], Sabine Van Huffel[1,2]

[1]KU Leuven, Stadius Center for Dynamical Systems, Signal Processing and Data Analytics, Belgium

[2]imec, Leuven, Belgium

Keyword(s): biosignals – medical/clinical engineering

1. INTRODUCTION

Cardiac arrhythmic diseases are considered as the number one cause of death all over the world. Any deviation from the normal conduction of the electrical impulses of the heart results in irregular heartbeats in the electrocardiogram (ECG) signal. Classification of abnormal heartbeats can help identify the cardiac arrhythmias. As it is expensive and time-consuming for manual identification of irregular heartbeats, automatic detection techniques have been developed over the last decades. In these traditional methods, ECG is represented as a vector, and time-domain based morphological features have been extracted directly from the ECG signal [1-3]. A tensor representation with a suitable tensor decomposition provides certain advantages [4]. In this work, a discrete wavelet transform (DWT)-based multiscale tensor algorithm is proposed to detect the irregular heartbeats of 12-lead ECG system.

2. MATERIALS AND METHODS

In this work, a subset consisting eleven of records of five patients from the St.-Petersburg Institute of Cardiological Technics (INCART) 12-lead Arrhythmia Database is considered. The database also contains the heartbeat annotations (R-peaks) for each record.

After baseline wander removal using a digital Butterworth high-pass filter from each ECG signal, the 12-lead ECG data is reshaped into a third-order tensor by juxtaposing frontal slices where each frontal slice represents a heartbeat of all leads. Then the 1-D DWT with 'L' decomposition level is applied along the mode-2 fibers. The DWT grossly segments the morphological features into different subbands. The MLSVD is then applied to all subband tensors. The parameters obtained from mode-2 and mode-3 factor matrices along with mode singular values are used to classify irregular heartbeats from normal ones.

3. RESULTS AND DISCUSSION

The performance of the proposed method is applied to the subset of INCART database that comprises 26482 normal and 1715 abnormal heartbeats. The selected parameters from multiscale subband tensors ($\mathcal{D}_5$-$\mathcal{D}_2$) are statistically different for normal and irregular heartbeats. This is because the morphological segments, due to the change in heartbeat shape, appear in different subbands depending on their frequency content.

4. ACKNOWLEDGMENT

This work was supported by ERC Advanced Grant: BIOTENSORS (nº339804). This paper reflects only the author's views and the Union is not liable for any use that may be made of the contained information.

References

[1] Chazal, P.D. et al. Automatic classification of heartbeats using ECG morphology and heartbeat interval features. *IEEE Transactions on Biomedical Engineering,* 51(7), 1196-1206, 2004.

[2] Tsipouras, M.G. et al. An arrhythmia classification system based on the RR-interval signal. *Artificial Intelligence in Medicine*, 33(3), 237-250, 2005.

[3] Lin, C.C. and Yang, C.M., Heartbeat Classification Using Normalized RR Intervals and Morphological Features. *Mathematical Problems in Engineering,* 2014.

[4] Sidiropoulos N. et al. Tensor Decomposition for Signal Processing and Machine Learning, *IEEE Transactions on Signal Processing*, 65(13), 3551-3582, 2017.

EPILEPTIC SEIZURE DETECTION BASED ON WRIST PHOTOPLETHYMOGRAPHY (PPG): DETECTION OF NOISE SEGMENTS

K. Vandecasteele[1,2*], J. Lazaro[1,2], W. Van Paesschen[3], S. Van Huffel[1,2] , B. Hunyadi[1,2]

[1]KU Leuven, Department of Electrical Engineering (ESAT), STADIUS Center for Dynamical Systems, Signal Processing and Data Analytics, Leuven, Belgium

[2]Imec, Leuven, Belgium

[3]KU Leuven, University Hospital, Department of Neurosciences, Leuven, Belgium

Keyword(s): biosignals

1. INTRODUCTION

The aim of the global project is to develop a wearable seizure detection system based on the integration of Electroencephalogram and Cardiorespiratory information. In a first step, the Heart Rate (HR) is investigated measured by wrist-worn Photoplethysmography (PPG). A disadvantage of PPG is the presence of motion artifacts [1], which will lead to poor specificity in seizure detection. In order to reduce these false alarms, the artefacted segments should be detected and later reconstructed.

2. MATERIALS AND METHODS

The data, used in this experiment, consists of 24-hour recordings of 17 patients, recorded in UZ Gasthuisberg with Empatica E4 (wrist PPG and triaxial Accelerometry (ACM)) and Faros (ECG). The data is split in 7s segments. Each segment is labeled as clean or artefacted by quantifying and comparing the HR extracted from ECG (reference) with the HR from PPG. For each segment, variance, first-/second-/third-largest peak of the spectrum, and spectral Shannon entropy are extracted in addition to 8 other features proposed in literature. Moreover, 20 ACM-derived features are calculated. A linear least-squares support-vector machine is proposed to classify the segments as a clean or artefacted segment within a leave-one-patient-out approach. A backwards wrapper is applied for feature selection on PPG- and ACM-derived features.

3. RESULTS AND DISCUSSION

In Table 1 the sensitivity (Sens), specificity (Spec) and Accuracy (Acc) are shown (Average ± standard value) for PPG-, ACM- and all features. Adding the ACM features to the classification does not increase the performance. The reason is that the PPG signal has already enough information on itself. By using only the ACM features, a low sensitivity is obtained. This is due to the fact that not all artefacts are caused by wrist motion, for example subtle finger motion.

An automated artefact detection method for PPG data is developed. For this dataset, the ACM features do not improve the performance, suggesting that ACM recording could be avoided from the point of view for detecting artefacts in PPG signals during daily life.

Table 1: Classification performance

	PPG	ACM	PPG+ACM
Sens [%]	85.50 ± 8	58.04 ± 18	85.50 ± 7
Spec [%]	91.84 ± 5	93.01 ± 4	92.36 ± 4
Acc [%]	90.33 ± 2	76.23 ± 11	90.23 ± 3

References

[1] Petterson, M.T. et al. The effect of motion on pulse oximetry and its clinical significance. *Anesthesia & Analgesia*, 105(6), S78-S84, 2007.

A TOOL FOR AUTOMATIC HEARTBEAT CLASSIFICATION IN AMBULATORY ECG

Amalia Villa Gómez[1,2*], Bert Vandenberk[3], Leuken Rojas Hernández[4], Alexander Alexeis Suárez León[1,5], Carlos R. Vázquez Seisdedos[6], Rik Willems[3], Sabine Van Huffel[1,2]

[1]KU Leuven, Department of Electrical Engineering (ESAT), STADIUS Center for Dynamical Systems, Signal Processing and Data Analytics, Leuven, Belgium
[2]IMEC, Leuven, Belgium
[3]Department of Cardiovascular Sciences, University of Leuven, Leuven, Belgium
[4]Cardiology Service, Hospital Provincial Saturnino Lora, Santiago de Cuba
[5]Department of Biomedical Engineering, Universidad de Oriente, Cuba
[6]Centre for Neuroscience Studies, Images and Signal Processing, Universidad de Oriente, Cuba.

Keyword: biosignals

1. INTRODUCTION

Sudden cardiac death (SCD) is one of the most important causes of natural mortality in the world. Researchers are trying to identify changes in the electrical activity of the heart that could predict the risk of this cardiac arrest. One of the approaches considered for this aim is the analysis of heart rate variability (HRV) [2], for which a Holter test is usually performed. The recorded signal is analyzed to obtain an automatic measurement. Since the analysis of HRV is only possible in normal sinus rhythms, heartbeat classification is required before it can be performed.

This HRV-based approach for SCD prediction is currently being investigated in the Cardiology Service of Hospital Provincial Saturnino Lora, from Santiago de Cuba (Cuba). Although the currently used Holter monitor includes software for automated heartbeat classification, its performance can still be significantly improved. The ECG signals are characterized by a low signal-to-noise ratio, which leads to a high number of errors in the automated diagnosis. These errors require the doctors to carefully correct the automatic analysis manually afterwards, which is time consuming.

The aim of this work is to present a software tool for unsupervised heartbeat classification. The software was adapted to enable automated labelling of the heartbeats, and with it, a new dataset was created. This challenging dataset will allow to test and compare the performance of a variety of heartbeat classification algorithms.

2. MATERIALS AND METHODS

The classification tool was developed in MATLAB. After a pre-processing stage, features are extracted to characterize each heartbeat.

A morphology approach is considered, using the 10 highest components of the Discrete Cosine Transform (DCT) of each heartbeat as its compressed description. These features are fed into a classifier which labels the heartbeats as normal or abnormal. The classifier is based on trimmed k-means [1], which allows to detect outliers corresponding to artefacts and irregular heartbeats.

3. RESULTS AND DISCUSSION

The outcome of this work is an automatic heartbeat classification tool, discriminating normal from irregular heartbeats. This function will be part of a toolbox developed by our research group, which combines artefact detection and heartbeat classification.

Besides the diagnostic tool, annotation software is developed, which allows fast labelling of heartbeats. Indeed, thanks to the above-mentioned first classification, only a few additional corrections are required by a cardiologist.

This tool is used to label signals recorded by the Holter monitor in the Hospital Provincial Saturnino Lora. This dataset will be used as test set for assessing the robustness of heartbeat classification algorithms, in particular in the presence of noise and artefacts.

References

[1] García-Escudero, L.A. et al. A general trimming approach to robust cluster analysis. *The Annals of Statistics*, 1324-1345, 2008.

[2] Lombardi, F. et al. Sudden cardiac death: role of heart rate variability to identify patients at risk. *Cardiovascular research,* 50(2), 210-217, 2001.

A REVIEW ON WEARABLE SENSORS FOR AGE-RELATED FRAILTY

Yiyuan Zhang[1,2*], Wei Chen[3], Bart Vanrumste[1,2]

[1]eMedia Research Lab, Campus Group T, KU Leuven, Belgium

[2]STADIUS - IMEC, Department of Electrical Engineering (ESAT), KU Leuven, Belgium.

[3]Center for Intelligent Medical Electronics, School of Information Science and Technology, Fudan University, China

Keywords: biosignals

1. INTRODUCTION

In Europe and China, the proportion of older adults (aged over 60 years old) is continuously raising, hence also the number of persons with aging-related frailty [1]. Therefore, self-reliance assessment is essential to older individuals. The object of this review is to analyze modern sensor devices (especially wearable ones) which can be used for diagnosing and following-up different varieties of physical activities which would be the symptoms of frailty.

2. MATERIALS AND METHODS

The literature search is carried out regarding to the objective mentioned above. World Health Organization (WHO) website, Google Scholar website and PubMed online database were selected as the resources.

According to [2], age-related frailty is categorized into five types: mobility, hearing, vision, cognitive impairment and urinary incontinence. Among them, mobility impairment is focused on this review. For the reason that physical activity is significantly associated with mobility impairment, surveys of activity monitoring using wearable sensors are discussed in the following section.

3. RESULTS AND DISCUSSION

3.1 Results

Five different types of activity, monitored features and applied sensors are illustrated in Table 1. ACM represents accelerometer, GRS for gyroscope and MAG for magnetometer.

3.2 Discussion

Although wearable sensors have been widely applied in activity monitoring, there are still drawbacks of the present research. Firstly, most experiments were conducted in the laboratory so that their feasibility in the natural environment needs to be proved. Secondly, most researchers focused on the recognition of limited types of activities, neglecting the quality level. Therefore, further research in more types of activities and the quality of the performed activities are needed.

Table 1. Monitored Activities and Applied Sensors

Activity Type	Feature	Sensors
Physical Activity	Sitting	1. CDXL04M3 -ACM 2. Lifecorder -ACM 3. ViM sports memory-ACM 4. sensor nodes-ACM, GSR
	Lying	
	Standing	
	Walking	
	Turning	
	Climbing up/down stairs	
	Sleep/wake	
	Brush-teeth	
Drinking	Ambulation status	1.Affectiva Equivital EQ2 2. Hexoskin smart shirt- ACM
	Hand and wrist movement	iBeacon
Dietary	Movement recognition of the arms	MTi (XSens) - ACM, GRS, MAG
	Food preparation movements (hands)	ADXL330-ACM
House-keeping	Housekeeping tasks	OPAL-ACM, GRS,MAG
Dressing	Dressing failures	RFID sensors

References

[1] Metz, D.H. Mobility of Older People and Their Quality of Life. *Transp. Policy*, 7(2), 149-152, 2000.

[2] World Health Organization. China country assessment report on ageing and health, 2015

Sponsors & Exhibitors

Golden

`

Cochlear®

Medtronic

SIEMENS Healthineers

Silver

Nobel Biocare™